



Escola d'Enginyeria de Telecomunicació i
Aeroespacial de Castelldefels

UNIVERSITAT POLITÈCNICA DE CATALUNYA

TREBALL FINAL DE GRAU

TFG TITLE: Airframe study and design for ONAerospace eVTOL

DEGREE: Grau en Enginyeria de Sistemes Aeroespacials amb menció d'Aeronavegació

AUTHOR: Juan Pablo Pineda Sandia

ADVISOR: Fernando Mellibovsky Einstein

SUPERVISOR: Jaume Suriaca Alvarez

DATE: February 4, 2023

Títol: Estudi i disseny de la cèl·lula de l'aeronau per ONAerospace eVTOL

Autor: Juan Pablo Pineda Sandia

Director: Fernando Mellibovsky Einstein

Supervisor: Jaume Suriaca Alvarez

Data: February 4, 2023

Resum

Les últimes dècades, hi ha una demanda creixent d'aviació elèctrica per part de la societat a causa dels beneficis ambientals i econòmics que ofereix. Van aparèixer nous conceptes d'avions com els eVTOL. Aquests avions tenen les capacitats dels helicòpters: Enlairament i Aterratge Verticals. Per aquest motiu, ONAerospace està dissenyant un nou concepte d'avió, anomenat ONA Jet, que podria, principalment, cobrir les operacions de recerca i rescat, mèdiques i comercials. L'ONA Jet s'acciona amb motors elèctrics i té capacitats VTOL. No obstant això, en creuer utilitza ales convencionals per generar sustentació. En aquest projecte s'estudiarà i dissenyarà la cèl·lula, concretament la forma del cos.

L'objectiu de disseny d'aquest treball és definir una solució que produeixi almenys el 25% de la sustentació total de l'avió en condicions de creuer amb una velocitat de pèrdua de 35 m/s. Això comportaria una disminució total de l'envergadura alar, reduint així el pes i permetria a l'aeronau aterrar a l'actual infraestructura VTOL.

S'ha dut a terme el disseny del cos de l'aeronau seguint procediments estàndard de disseny de l'aeronau, primer definint les mesures internes de la cabina i després, la forma exterior.

La validació dels resultats i els estudis paramètrics s'han fet mitjançant ANSYS, una eina CFD (Computational Fluid Dynamics) que permet la validació del disseny en condicions reals del túnel de vent o de vol. Tanmateix, s'ha validat només en 2D a causa de les limitacions de la versió del programa disponible.

Finalment, s'ha presentat un disseny vàlid, aconseguint els requisits prèviament definits. Tanmateix, s'hauran de reconsiderar o perfeccionar diverses consideracions i paràmetres de disseny en estudis posteriors per tal de maximitzar el rendiment total de l'avió.

Title: Airframe study and design for ONAerospace eVTOL

Author: Juan Pablo Pineda Sandia

Advisor: Fernando Mellibovsky Einstein

Supervisor: Jaume Suriaca Alvarez

Data: February 4, 2023

Overview

During the last decades, there has been an increasing demand for electric aviation from society due to the environmental and economic benefits it offers. New aircraft concepts have appeared such as the eVTOLs. These aircrafts have the helicopters capabilities: Vertical Take-Off and Landing. For that reason, ONAerospace is designing a new aircraft concept, called ONA Jet. This concept could cover search and rescue, medical and commercial operations. The ONA Jet is powered by electrical motors and has VTOL capabilities. However, when cruising it uses conventional wings to generate lift. This project studies and designs the airframe, specifically the body shape.

The design objective of this work is to define a body shape solution which produces at least 25% of the total aircraft lift in cruise conditions with a stall speed of 35 m/s. This would lead to a decrease of the total wing span, so reducing weight as well as enabling the aircraft to land in the current VTOL infrastructure.

The body of the aircraft has been designed following standard aircraft designing procedures, first defining the cabin measures and then, the shape itself.

The results validation and the parameter studies have been done with ANSYS, a CFD (Computational Fluid Dynamics) tool that allows the design validation in real wind tunnel or flight conditions. However, it has been validated just in 2D due to software version limitations.

Finally, a valid design has been presented, achieving the previously defined requirements. However, several design considerations and parameters will have to be reconsidered or refined in subsequent studies in order to maximize the total airplane's performance.

A mis tutores Jaume Suriaca, Núria Anducas y Fernando Mellibovsky.
Por darme la oportunidad de participar en este proyecto tan ambicioso.
También al resto del equipo de ONAerospace por la comunicación y
profesionalidad, en especial al departamento de aerodinámica.

INDEX

INTRODUCTION.....	1
CHAPTER 1. DESIGN OBJECTIVES.....	4
1.1. eVTOL evolution	4
1.2. Objectives of the design	5
CHAPTER 2. THEORETICAL AERODYNAMICS CONCEPTS	6
2.1. Fundamental aerodynamic concepts	6
2.2. Fuselage aerodynamics factors.....	8
2.3. Airfoil parameters	10
2.4. Dimensionless parameters.....	11
CHAPTER 3. FUSELAGE DESIGN PARAMETERS.....	16
3.1. Configurations and operations	16
3.2. Type of fuselage shape.....	17
3.2.1. The Frustum-Shaped Fuselage.....	18
3.2.2. The Pressure Tube Fuselage.....	18
3.2.3. The Tadpole Fuselage.....	19
3.3. Internal Dimensions of the Fuselage design.....	21
3.4. External shape.....	23
3.5. Flight deck design (Visibility).....	27
CHAPTER 4. METHODOLOGY.....	30
4.1 SolidWorks.....	30
4.2 Ansys.....	30
CHAPTER 5. BODY DESIGN	34
CHAPTER 6. BODY AERODYNAMIC STUDY.....	40
CONCLUSION	54
BIBLIOGRAPHY.....	55

List of Abbreviations

- **AFM:** Aircraft Flight Manual
- **AoA:** Angle of Attack a.k.a. α
- **CAD:** Computer-Aided Design
- **CAE:** Computer-Aided Engineering
- **CAM:** Computer-Aided Manufacturing
- **Cd:** Drag coefficient
- **CFD:** Computational Fluid Dynamics
- **Cl:** Lift coefficient
- **Cm:** Coefficient of the pitching moment
- **eDFAN:** Electrical Ducted Fan
- **eVTOL:** Electric Vertical Take-Off and Landing
- **FEA:** Finite Element Analysis
- **HEMS:** Helicopter Emergency Medical Service
- **IFR:** Instrumental Flight Rules
- **LE:** Leading Edge
- **MAC:** Mean Aerodynamic Chord
- **MCG:** Mean Center of Gravity
- **MEDEVAC:** Medical evacuation
- **MTOW:** Maximum Take-Off Weight
- **OEW:** Operating Empty Weight
- **PAX:** Passengers
- **Re:** Reynolds Number
- **SAR:** Search and Rescue
- **TE:** Trailing Edge
- **VFR:** Visual Flight Rules
- **Vstall:** Speed at which the aircraft stalls
- **VTOL:** Vertical Take-Off and Landing

Introduction

The aviation and aerospace industries are constantly evolving and looking for new technologies to satisfy society's needs. In fact, last decades the demand for electric aviation has been increased due to the environmental and economic benefits it offers.

Traditional aircraft are a major source of carbon emissions, and the use of electric propulsion systems can significantly reduce it. In addition, electric aircraft have the potential to reduce operating costs as well due to the lower cost of electricity compared to fossil fuels.

On the other hand, last decades we have seen an increased demand for a short and mid-range travels transport. Then, the concept of VTOL (vertical take-off and landing) appears; it is considered the best to implement it in the cities as well as using it for certain kind of operations.

Merging these two society's demands, the eVTOL concept is designed. This electrical Vertical Takeoff and Landing aircraft, whose goal is to transport people in short/mid-range routes as well as including the vertical mobility in urban areas, profits from the current infrastructures, for instance the heliports.

Then, in order to satisfy the society needs, ONAerospace is developing an eVTOL aircraft called ONA Jet with the main three kinds of different configurations: search and rescue, commercial transport, and medical aids.

This document deals with the airframe study and design of the ONA Jet, specifically the aerodynamics aspect. First, introducing the reader to the subject of eVTOL technology as well as defining the objectives of this design; second, concepts of aerodynamics and defining the body going through the airframe parameters. Finally, an analysis of the simulations carried out with Ansys.

Chapter 1. Design Objectives

1.1. eVTOL evolution

The concept of vertical takeoff and landing (VTOL) aircraft dates back to the early 20th century, but the first practical VTOL aircrafts were developed in the 1950s and 1960s. These early VTOL aircrafts were typically powered by jet engines and were used mainly by military forces for tasks such as search and rescue, transport, and surveillance. [1]

The first VTOL aircraft was the Focke-Wulf Fw 61 (figure 1.1), designed and built by German engineer Heinrich Focke in 1936. It was a helicopter that was capable of taking off and landing vertically, as well as flying horizontally like a traditional aircraft. The Fw 61 made its first flight in 1936 and was the first aircraft to demonstrate true VTOL capabilities. It was also the first aircraft to be controlled entirely by a pilot using a joystick, rather than through the use of pedals and a control wheel. The Fw 61 was a pioneering aircraft that paved the way for the development of other VTOL aircraft, including helicopters and tiltrotors.



Fig.1.1 Focke-Wulf Fw 61 in flight [3]

In the 21st century, there has been a growing interest in developing electric VTOL (eVTOL). This aircraft is designed to take off and land vertically, like a helicopter. However, unlike a helicopter, an eVTOL aircraft uses electric motors rather than mechanical rotors to generate lift, which makes them quieter [2], more efficient, and more environmentally friendly. Some eVTOL aircraft are also designed to be autonomous, meaning they can be operated without a pilot on board. These features make eVTOL aircraft well-suited for use in urban environments, where they can be used for transportation, delivery, and other purposes.

In recent years, humanity became aware of climate change and its causes, CO2 emissions among others. That is why there has been this growing interest in developing eVTOL aircraft for civilian use, it is because it has the potential to

revolutionize transportation by providing a faster, more convenient, and more environmentally friendly alternative to cars and other ground-based modes of transportation. Many companies and startups are currently working on developing and bringing eVTOL aircraft to market, and it is expected that these aircraft will start to become more common in the coming years. At the beginning just big companies like Airbus [5], Boeing [4], NASA [6], etc. opted for this solution. Nowadays, different companies which began as start-ups, are pioneers in this concept; these are Joby Aviation [7], Lillium [8], Volocopter [9] and soon ONAerospace.

1.2. Objectives of the design

In order to define the objectives, it is needed first to know the key factor that affects the aerodynamics of an aircraft: shape (wing & body), size, Angle of Attack (AoA) and speed. The process to follow is shown in the figure below:



Fig.1.2 Elementary outline of an aircraft design process [12]

As mentioned in the overview, our duty is to study and designing the ONA Jet airframe with certain requirements: producing the 25% of the total lift with a V_{stall} of 35 m/s using the cruising configuration.

This computation will be carried out by using the software Ansys Student Fluent [10], which entails a limitation in terms of software tools. Even so, this computational study will be done by considering the aircraft's body such an airfoil, i.e., in 2 dimensions. Despite this, a volume would be designed in SolidWorks [11] in order to assembly the part together with the main wings and the V-tail in a future, and do a complete aerodynamic study of the ONA Jet.

So, right now the ONA Jet is in the conceptual and preliminary design as shown in figure 1.2.

Chapter 2. Theoretical aerodynamics concepts

In this chapter it will be explained the fundamental aerodynamics concepts, fuselage aerodynamic factors and the airfoil parameters.

2.1. Fundamental aerodynamic concepts

First, we have to define the airflow. The movement of air around and through an object is known as airflow. The characteristics of airflow, such as its velocity, pressure, and density, can have a significant effect on the aerodynamic performance of an object (Fig.2.1).

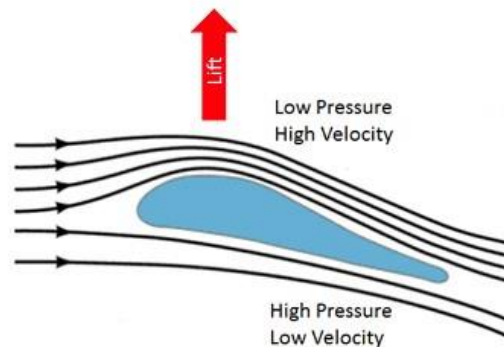


Fig.2.1 Airflow passing through an airfoil [12]

Furthermore, when the airflow interacts with the airfoil, the aerodynamic forces appear (Lift and Drag) and the Bernoulli's Principle must be defined.

Bernoulli's principle states that as the velocity of a fluid increases, the pressure of the fluid decreases. This relationship is used to explain how lift is generated on an object, such as an airplane wing. According to Bernoulli's principle, since the air passing over the top of the wing travels faster than the air passing under the wing, the air above the wing has lower pressure than the air below the wing, resulting in lift.

Lift is the force that acts perpendicular to the direction of airflow and helps to support the weight of an object. Lift is generated by the difference in pressure between the top and bottom surfaces of an object, and it is what allows an airplane to take off and fly. Therefore, the total pressure lift is the integral of the pressure over the airfoil surface, in the direction perpendicular to the airfield flow, see the equation 2.1 [14]:

$$L = \oint (p \cdot \hat{n}) \cdot \hat{k} \cdot dS \quad (2.1)$$

Where L is the Lift, k is the vertical unit vector normal to the freestream direction, p is the Pressure, n is the normal unit vector pointing into the wing and dS is the body's surface that is being studied into infinitesimally small parts.

However, the equation 2.1 does not take into consideration the skin friction forces due to the huge differences between them and the pressure forces, so, they are neglected.

Now, the lift coefficient (C_l) has to be defined because it relates the lift generated by a lifting body to the fluid density around the body, the fluid velocity and an associated reference area.

The C_l is a dimensionless number that represents the lift generated by an object, such as an airplane wing, in relation to the size of the object and the speed and density of the air. It is defined as the lift generated by an object divided by the product of the air density, the velocity of the air, and the reference area of the object. If the lift is isolated from the description above, we would obtain an alternative equation for the lift, see equation 2.2 [14]:

$$L = \frac{1}{2}\rho v^2 S C_l \quad (2.2)$$

The coefficient of lift can be used to predict the lift generated by an object under different conditions, such as different speeds or densities of air. It is an important factor in the design and analysis of objects that are affected by lift, such as aircraft, automobiles, and sports equipment. The coefficient of lift can be affected by a number of factors, including the shape of the object, the angle of attack, and the roughness of the surface.

From equation 2.2 we can extract the parameters to modify in order to gain more or less lift. The ones which are directly proportional to the lift are: the wing surface, the lift coefficient obtained from the shape of the airfoil profile and the density of the fluid. I.e., when increasing them, the lift will do so, and vice versa when decreasing. On the other hand, there is the speed, which increases the lift quadratically.

For the equation 2.1 there is a neglect of the skin friction forces because were too small compared to lift so negligible. However, it does not mean there is no drag, which is caused by viscous forces of the fluid as well as pressure forces.

In fluid dynamics, drag is a force that acts against the motion of a body as it moves through a fluid. The magnitude of the drag force depends on several factors, including the shape and size of the body, the density and viscosity of the fluid, and the velocity of the body relative to the fluid. The direction of the drag force is always opposite to the direction of motion [15]. Following the same dimensional analysis done for Lift but for Drag the equation 2.3 is obtained:

$$D = \frac{1}{2}\rho v^2 S C_d \quad (2.3)$$

There are two main types of drag: parasitic drag and lift-induced drag.

- **Parasitic drag:** is the resistance that a body experiences as it moves through a fluid and includes forms such as skin friction drag and wake pressure drag.
- **Lift-induced drag:** is a result of the lift force that is generated by a 3D body as it moves through a fluid and is caused by the formation of 3D fluid flow around the body.

$$C_d = C_{d_p} + C_{d_i} \quad (2.4)$$

To minimize drag, it is important to design the shape of the body to be as streamlined as possible, with a smooth, continuous surface and a minimum of protruding features. Other techniques to reduce drag include the use of materials with low drag coefficients and the use of flow control devices such as vortex generators and winglets.

Another important phenomenon to be tackled is the downwash. It is a type of aerodynamic effect caused by an aircraft flying through the air. As air passes over the wings of an aircraft, it is deflected downward due to the shape of the wings and the force of the air passing over them. The downward force creates a "downwash" effect, which causes the air behind the aircraft to be pushed downward as well.

This effect is most noticeable when an aircraft is flying at a high speed and has a large wing area.

2.2. Fuselage aerodynamics factors

The fuselage of an aircraft is the main body of the aircraft, which typically houses the crew, passengers, and cargo. Aerodynamics plays a crucial role in the design of the fuselage, as it affects the overall performance and efficiency of the aircraft.

There are several factors that are considered in the aerodynamic design of an aircraft fuselage, including:

- **Shape:** The shape of the fuselage affects the drag and lift forces that act on the aircraft. A streamlined shape can reduce drag and improve the aircraft's performance, while a more bluff or boxy shape can increase drag and reduce performance.

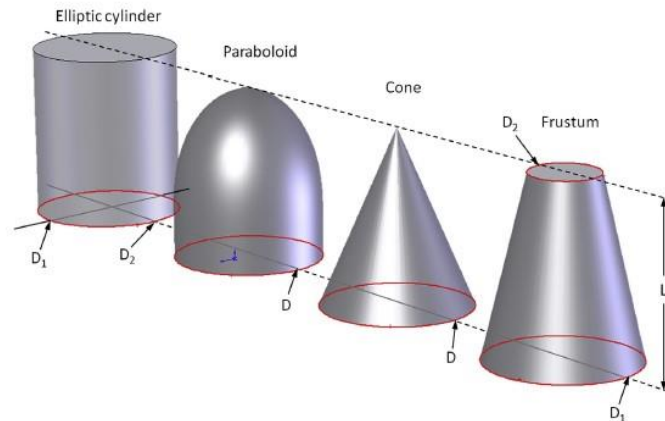


Fig.2.2 Elementary solids with the same height [12]

One important aspect of fuselage aerodynamics is the cross-sectional shape of the fuselage. A circular cross-section will produce the least amount of friction, but is not practical for most aircraft due to the lack of interior space. A more common cross-sectional shape is an ellipse, which is more efficient than a rectangle of the same area.

- **Size:** The size of the fuselage plays a role in the aircraft's weight and can also affect its aerodynamics, with larger fuselages generally experiencing more drag than smaller ones.
- **Surface finish:** The smoothness of the fuselage surface can also impact the amount of drag experienced by the aircraft. In the same way, a rough surface may increase drag. An example of this could be windows, doors, and antennas. These features can create local regions of high or low pressure that can affect the overall airflow around the fuselage. To reduce drag, the fuselage is often designed with features such as streamlined fairings over joints and openings, and a tapered or rounded nose and tail.
- **Positioning of other aircraft components:** The position and orientation of other components, such as the wings and engines, can also affect the aerodynamics of the fuselage. For example, a wing mounted high on the fuselage may create a more streamlined shape and reduce drag.

Overall, the aerodynamics of the fuselage is an important factor in the design and performance of an aircraft. By carefully considering these factors, the aim is to design an aircraft that is efficient, stable, and capable of flying at low speeds as well as high speeds.

2.3. Airfoil parameters

An airfoil is a shaped surface designed to produce lift when it moves through a fluid medium, such as air. There are several important parameters that are used to describe the geometry and performance of an airfoil. These parameters include (figure 2.3):

- **Camber:** This is the curvature of the airfoil from top to bottom. A cambered airfoil has a curved shape, with the top of the airfoil being higher than the bottom. This type of airfoil is often used in applications where lift is required, such as in aircraft wings.
- **Chord:** This is the distance from the leading edge to the trailing edge of the airfoil, measured along the chord line. The chord line is a straight line drawn from the leading edge to the trailing edge.
- **Thickness:** This is the distance from the upper surface to the lower surface of the airfoil, measured along a line perpendicular to the chord line. A thicker airfoil is generally more efficient at producing lift, but is also more susceptible to drag.
- **Angle of attack:** This is the angle between the chord line of the airfoil and the direction of the fluid flow. Increasing the angle of attack increases the lift produced by the airfoil, but also increases the drag.
- **Leading edge radius:** This is the radius of the curve at the leading edge of the airfoil. A smaller leading-edge radius can help to reduce the amount of shock waves and separation that occur at high angles of attack, improving the performance of the airfoil.
- **Maximum thickness:** This is the maximum thickness of the airfoil, measured along a line perpendicular to the chord line. The maximum thickness is often used to describe the shape of the airfoil and can have a significant effect on its performance.
- **Mean camber line:** This is a line drawn through the points of maximum camber on the top and bottom surfaces of the airfoil. The mean camber line is used to describe the overall shape of the airfoil.
- **Point of maximum camber:** This is the point on the mean camber line where the camber is greatest. The location of the point of maximum camber can have a significant effect on the lift and drag characteristics of the airfoil.

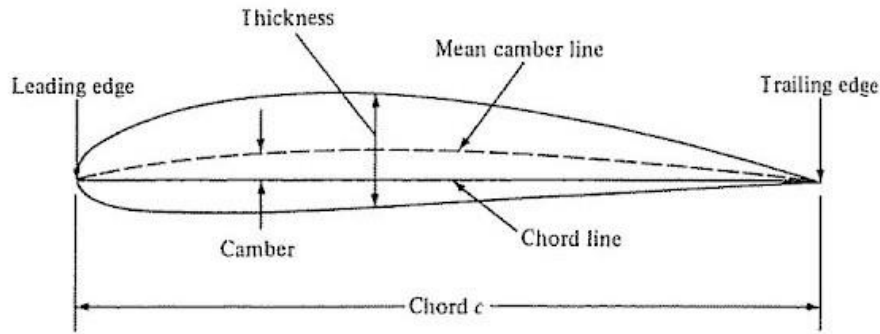


Fig.2.3 Airfoil parts [19]

In conclusion, the airfoil parameters of camber, chord, thickness, angle of attack, leading edge radius, maximum thickness, mean camber line, and point of maximum camber are all important factors that can affect the performance of an airfoil. Understanding these parameters is essential for designing and analyzing the performance of airfoils in various applications.

2.4. Dimensionless parameters

There are several dimensionless parameters that are used to describe the flight regime and performance of an airfoil. These parameters are useful for comparing the performance of different airfoils, as they take into account the size and shape of the airfoil, as well as the properties of the fluid in which it is operating. Some of the most commonly used dimensionless parameters for an airfoil are:

- **Reynolds number:** This is a measure of the relative importance of viscous forces to inertial forces in the fluid flow around the airfoil. It is defined as:

$$Re = \frac{(\text{density} \times \text{velocity} \times \text{chord})}{\text{viscosity}} \quad (2.5)$$

A high Reynolds number indicates that the inertial forces are dominant and the flow is more likely to be turbulent, while a low Reynolds number indicates that the viscous forces are dominant and the flow is more likely to be laminar.

- **Lift coefficient:** This is a measure of the lift force produced by the airfoil, normalized by the dynamic pressure of the fluid flow and the surface area of the airfoil. It is defined as:

$$Cl = \frac{\text{Lift force}}{\text{dynamic pressure} \times \text{surface area}} \quad (2.6)$$

- **Drag coefficient:** This is a measure of the drag force produced by the airfoil, normalized by the dynamic pressure of the fluid flow and the surface area of the airfoil. It is defined as:

$$C_d = \frac{\text{Drag force}}{\text{dynamic pressure} \cdot \text{surface area}} \quad (2.7)$$

- **Oswald efficiency factor:** This is a measure of the effectiveness of the airfoil in producing lift. It is defined as:

$$e = \frac{C_L^2}{\pi \cdot AR \cdot (C_D - C_{D0})} \quad (2.8)$$

Where e is the Oswald efficiency factor, C_{D0} is the zero-lift drag coefficient of the airfoil, C_L is the coefficient of lift of the airfoil.

The Oswald efficiency factor is a useful parameter for comparing the overall performance of different airfoils. A high Oswald efficiency factor indicates that the airfoil is able to produce lift with a low amount of drag, while a low Oswald efficiency factor indicates that the airfoil is less efficient at producing lift.

- **Pitching moment coefficient:** It is a dimensionless coefficient that relates the pitching moment (the moment about the aerodynamic center of an airfoil or wing) to the dynamic pressure of the fluid flow and the wing chord.

For an aircraft to be stable, the pitching moment coefficient must have negative slope with respect to CG at the normal operating angles of attack. This means that as the angle of attack increases, the pitching moment coefficient should decrease, causing the nose of the aircraft to pitch down and return to its original attitude. This is known as a "stable" or "positive" static margin, and it ensures that the aircraft will naturally return to its trimmed condition if disturbed by a gust or other external disturbance. The value of C_m needed to achieve this stability depends on the design of the aircraft and its intended operating conditions.

Additionally, the aircraft should also have a positive dynamic stability, which means that the aircraft response to a disturbance should dampen out and return to the initial condition. This is achieved by having a negative value of the damping coefficient which is the derivative of C_m with respect to the pitch angular velocity. This shown below in the figure 2.5.

In conclusion, the dimensionless parameters of Reynolds number, lift coefficient, drag coefficient, and Oswald efficiency factor are all important factors that can be used to describe the performance of an airfoil. These parameters take into account the size and shape of the airfoil, as well as the properties of the fluid in which it is operating, and can be used to compare the performance. The performance is compared using the different graphs:

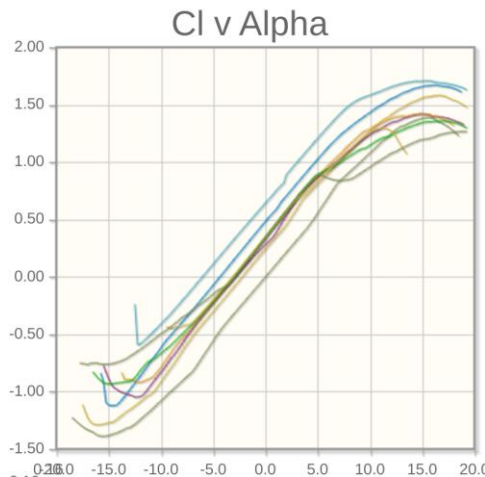


Fig.2.4 Cl vs AoA for different NACA [27]

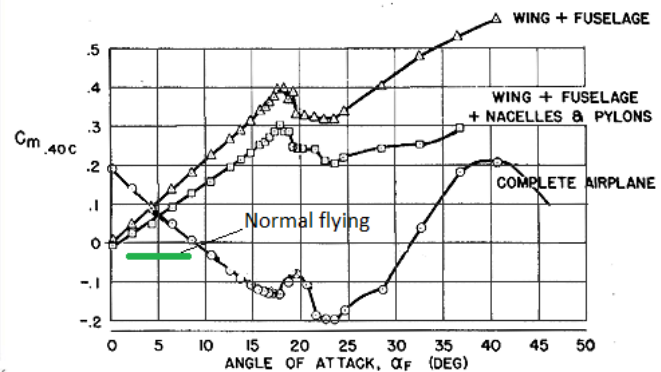


Fig.2.5 Cm vs AoA [28]

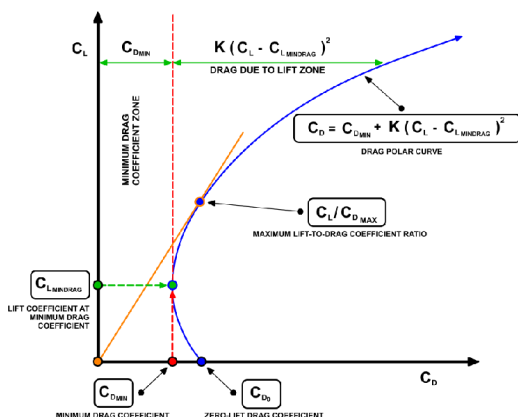


Fig.2.6 Cl vs Cd [29]

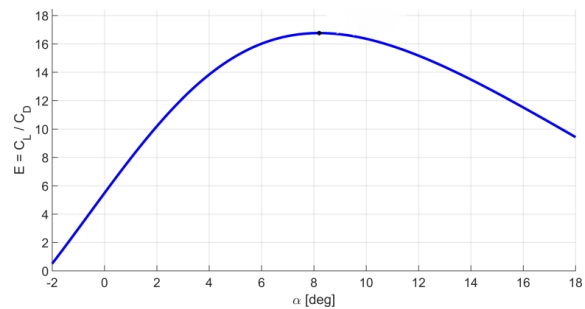


Fig.2.7 Cl/Cd vs AoA [30]

- Cl vs AoA:** As it is shown in figure 2.4, as the angle of attack of an airfoil or wing increases, so does the lift coefficient. However, at a certain point, the lift coefficient will reach a maximum value and then decrease as the angle of attack continues to increase. This is known as the stall angle, is typically around 15° . At the stall angle, the airflow across the upper cambered surface ceases to flow smoothly and in contact with the upper surface and separates, thus greatly reducing lift and increasing drag.

- **Cm vs AoA:** In figure 2.5, the graph shows how the pitching moment coefficient changes with the angle of attack. The lift on an airfoil is a distributed force that act at the center of pressure. However, as angle of attack changes there is movement of the center of pressure forward and aft. Depending on the position of the center of pressure with respect to the CG, the Cm will have a different value. For symmetric airfoils, the pitching moment coefficient is zero at zero angle of attack, and it becomes negative as the angle of attack increases. For cambered airfoils, the pitching moment coefficient is negative at zero angle of attack, and it becomes more negative as the angle of attack increases. The Cm (X_{cg}) vs AoA curve with a negative slope means that the pitching moment is always trying to bring the aircraft into the trim (equilibrium) condition. This is stable. A positive slope means the pitching moment is always trying to push the aircraft away from trim condition. This is unstable. [28]
- **Cl vs Cd:** It is shown in figure 2.6 how the drag coefficient increases as the lift coefficient increases. The slope of this graph is called the drag polar. It is a measure of the trade-off between lift and drag. The steeper the slope of the straight line from the origin to the polar curve, the higher the drag per lift unit, and the less efficient the wing is. This could be characterized as well by the aerodynamic efficiency, i.e., Cl divided by Cd.
- **Cl/Cd vs AoA:** In figure 2.7 is shown how the aerodynamic efficiency changes as the AoA increases. This graph enables us to find the AoA for an optimal aerodynamic efficiency. At low angles of attack, the aerodynamic efficiency will be high, as the lift-to-drag ratio is high. As the angle of attack increases and approaches the stall angle, the aerodynamic efficiency will decrease as the drag increases and the lift-to-drag ratio decreases.

Chapter 3. Fuselage design parameters

First the exposition of the requirements. As it is explained in this chapter, the ONA Jet will be designed for three main configurations: SAR, HEMS and commercial. In terms of internal space, the commercial one is the most restrictive because of its capacity. Then, the commercial operations requirements are shown below in table 3.1.:

Table 3.1. Requirements' table

Stall speed (V_{stall})	35 m/s
Cruise speed	89.44 m/s
MTOW	2950 kg
N° engines	3
Engines distribution	2 at the front and 1 incrustated at the tail
PAX	7
Crew (Just Pilot)	1
Seats	8
Aisle	1

In order to design the fuselage, it is crucial to remark first the operations and type of configurations. Once it is done, the internal dimensions of the fuselage sections must be defined. Then, the external dimensions and shape.

3.1. Configurations and operations

The ONA Jet is an e-VTOL aircraft concept that utilizes tiltable electrical motors and fixed motors for vertical takeoffs and landings. The goal of the aircraft is to perform similar tasks as traditional helicopters, and thus, it will have various configurations for different activities. The economic benefits of this aircraft instead of the helicopter is that the operation cost will decrease. It is due to fuel costs since the propulsion system relies on electricity and not on fuel. In terms of maintenance cost, it will decrease as well because the propulsion system will not induce as much vibrations as the fuel engines and it does not suffer as much pressure and high temperatures as conventional fuel engines; so, the maintenance checks will be simplified. Also, it is safer and more efficient since it does not dissipate as much energy. The aircraft will be designed specifically with three kinds of operations in mind:

- **SAR operations:** The Search and Rescue (SAR) operations are a service provided to the survivors of aircraft accidents as well as aircraft in distress and its crew. [21] This configuration means the ONA Jet is carrying survival equipment in order to rescue people (figure 3.1.).



Fig.3.1. SAR operation example [25]

- **HEMS operations:** HEMS means by Helicopter Emergency Medical Service. [22] The configuration for these operations will carry out medical operations such as MEDEVAC, i.e., medical evacuations (figure 3.2).



Fig.3.2. HEMS cabin example and the medical equipment

- **Commercial operations:** This operations' configuration will have a capacity of 7 passengers, and it will provide the service as an air taxi but with much lower costs as it is mentioned before.

3.2. Type of fuselage shape

The study will be focused in the cruise performance thus the principal type of fuselage from conventional aircraft will be studied: the Frustum-Shape fuselage (figure 3.3.), the Pressure Tube fuselage (figure 3.4.) and the Tadpole fuselage (figure 3.5.). [12]

3.2.1. The Frustum-Shaped Fuselage

The frustum-shaped fuselage is a type of aircraft fuselage design that features a tapered shape, similar to that of a frustum, which is a geometric shape that is similar to a cone or pyramid with the top cut off. This design is characterized by a wide front section that gradually tapers towards the rear.

It is common to manufacturers like Beechcraft, Cessna, and Piper. In figure 3.3 is shown this fuselage applied to a conventional aircraft such as the Piper PA-28 Cherokee.



Fig.3.3. Frustum Style Fuselage. Piper PA-28 Cherokee [31]

They are inexpensive to produce because they can be made from folded sheet metal riveted to frames, which produces a light and stiff structure. It is a drawback that they generate far more drag than tadpole fuselages. The configuration is the right choice for roomy, inexpensive, stiff, and strong fuselages, where drag is not an issue, but internal volume is. The frustum fuselage is ideal for utility transport aircraft. However, if the goal is an aerodynamically efficient aircraft, frustum-shaped fuselages are the wrong choice. Such fuselages are indicative of the aircraft design philosophy of yesteryear and, today, are primarily justified by reduced production costs.

3.2.2. The Pressure Tube Fuselage

A pressure tube fuselage is a type of aircraft fuselage design that uses a hollow tube or series of tubes to maintain the pressure inside the cabin. This design is characterized by a strong, lightweight structure that is able to withstand the high cabin pressures that are required for high-altitude flight. If the airplane is

pressurized, the cross-section is circular, as no geometry carries pressure loads more efficiently

This type of fuselage design is typically used on aircraft that fly at high altitudes, such as commercial aircraft. The design allows for a pressurized cabin, which allows the aircraft to fly at higher altitudes and provides a more comfortable environment for the crew and passengers.

The pressure tube fuselage (figure 3.4.) design also offers the advantage of being relatively simple and easy to construct, as the tube or series of tubes can be made from a variety of materials, such as aluminum or composite materials.

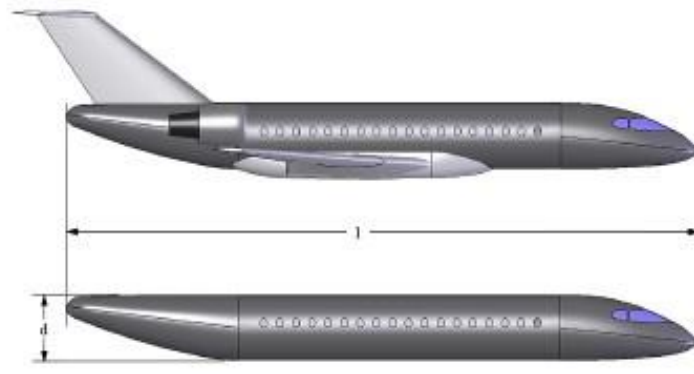


Fig.3.4. Pressure Tube Fuselage [12]

3.2.3. The Tadpole Fuselage

The tadpole fuselage is a type of aircraft fuselage design that is characterized by a streamlined shape that resembles a tadpole. It features a bulbous front section (the "head" of the tadpole) that gradually tapers towards the rear (the "tail" of the tadpole). This design is intended to reduce drag and improve aerodynamic efficiency.

This fuselage is more expensive to produce than frustum fuselages, in particular if made from aluminum as the geometry features compound surfaces that would call for expensive metal-forming processes. Their production can be achieved more economically using composites and this remains the primary method used for this purpose (figure 3.5.).



Fig.3.5. Tadpole Fuselage. Diamond DA20 C-1

Tadpole fuselages generate far less drag than the frustum kind for two primary reasons:

1. Their forward portion is shaped to sustain laminar boundary layer.
2. Their empennage shape results in as much as 30-40% less wetted area.

Similar to laminar airfoils, the front part of the body should produce favorable pressure gradients in all meridians even at incidences of about $\pm 10^\circ$. At the same time, the whole surface should be smooth and leak-free in order to avoid any disturbances to the laminar flow.

Behind the transition front it is favorable to contract the cross-section. On one hand, this reduces the wetted surface; on the other, it shifts the unavoidable pressure rise to the thinner parts of the turbulent boundary layer, which is a well-known principle of favorable boundary layer control.

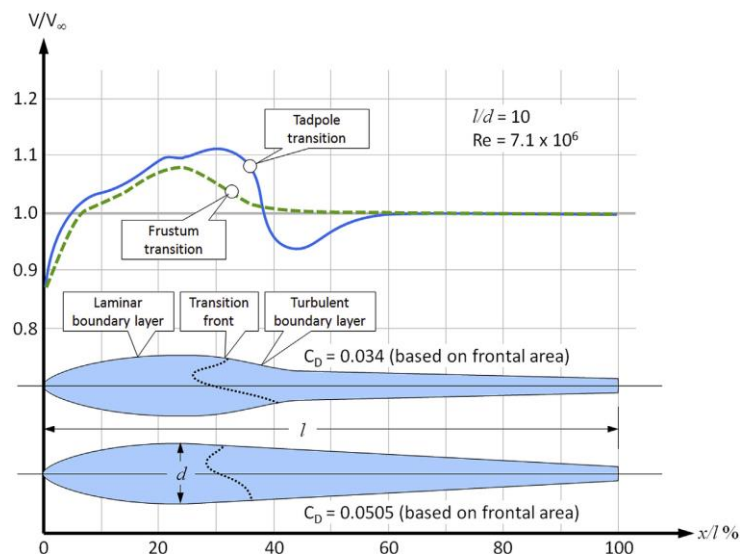


Fig.3.6. Frustum vs Tadpole transition from laminar to turbulent [12]

In figure 3.6 is shown the transition comparison of Frustum vs Tadpole using the same fineness ratio and Re . We can observe that the drag of the frustum is almost 49% larger than the drag of the tadpole fuselage, based on the frontal area.

3.3. Internal Dimensions of the Fuselage design

First, the frontal cross-section shape is tackled. It can be designed to either increase or decrease drag, depending on the desired performance characteristics. In our case, the desired option is the most aerodynamic efficient, so minimizing the drag as maximum as possible.

In figure 3.7 there is shown three different mid-section shapes. These are classical shapes we find in commercial aircraft and general aviation but we need to know which one is the ideal streamline shape.

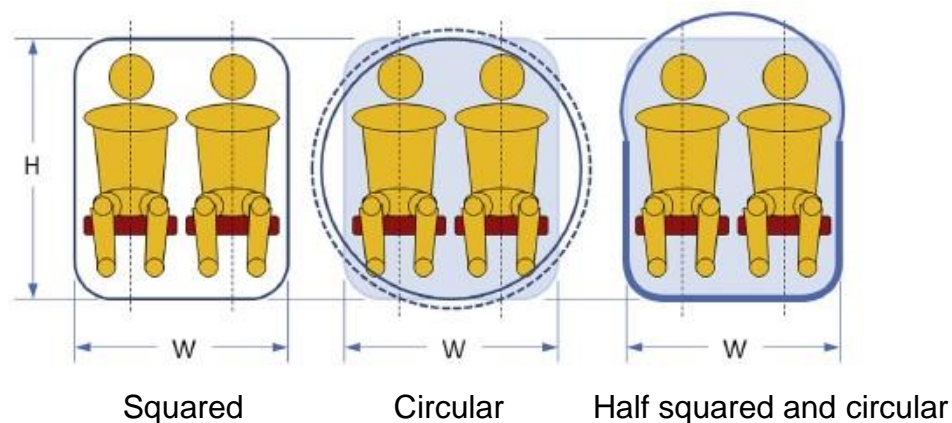


Fig.3.7. Frontal cross-section shapes [12]

Despite all of them have advantages and inconvenients, the circular mid-section is the chosen one. This shape, from the commercial configuration point of view, is the chosen for our aircraft for the following reasons:

- Structural design and manufacture are considerably simplified.
- It is possible to obtain an efficient internal layout with little loss of space.
- The flexibility of the seating arrangement is improved.
- Further development by increasing the length of the fuselage (stretching) is facilitated.

- The need of pressurizing, in a future advanced ONA Jet, is already taken into account with this shape since the structure suffers less than with other shapes.

Once the shape is chosen, the dimensions have to be defined.

		MALE AND FEMALE PHYSICAL CHARACTERISTICS						
		1st	5th	50th	95th	99th		
Stature	A	Male	63.1	64.8	69.1	73.5	75.2	in
			160.3	164.6	175.5	186.7	191.0	cm
	Female	58.4	60.2	64.1	68.4	70.1	in	
		148.3	152.9	162.8	173.7	178.1	cm	
Leg at 0°	L ₀	Male	17.4	18.2	19.8	21.7	22.4	in
			44.2	46.2	50.3	55.1	56.9	cm
	Female	15.7	16.4	18	19.8	20.6	in	
		39.9	41.7	45.7	50.3	52.3	cm	

Fig.3.8 Physical characteristics [12]

For the cabin height we look at the figure 3.8, taking the biggest case there is a maximum height of 1.91 m. However, in the commercial configuration, our aircraft design features an aisle, then, the dimensions would be 0.56 m wide, 1.09 m deep, and 1.93 m high. It is given to each passenger in order to let them to move around freely. As remark, for the length we will consider 1.6 m more for the passengers baggage; regarding the width, the aisle will measure 0.58 m.

We are dealing with an 8 people capacity distributed in 2 rows of 4 seats in each one. So, for the total cabin length it is multiplied 1.09 m by 4 which is the number of people by row (3.1), for the total cabin width it is multiplied 0.56 by 2, referring each row, plus the aisle width (3.2):

$$\text{Cabin Length} = 1.09 \times 4 + 1.6 = 5.96 \text{ m} \simeq 6 \text{ m} \quad (3.1)$$

$$\text{Cabin Width} = 0.56 \times 2 + 0.58 = 1.7 \text{ m} \quad (3.2)$$

$$\text{Cabin height} = 1.93 \text{ m} \quad (3.3)$$

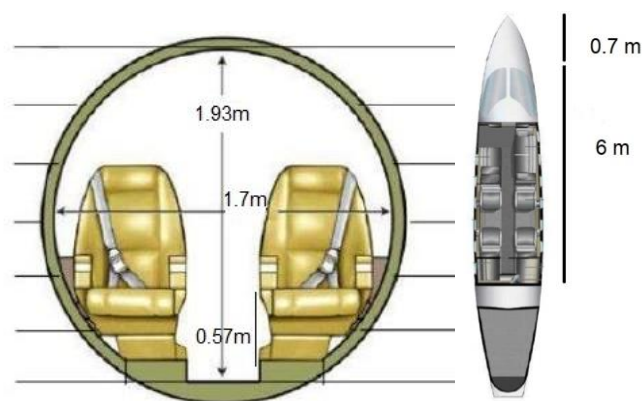


Fig.3.9 Cabin measurements

3.4. External shape

Now the external longitudinal cross-section has to be tackled. One common longitudinal cross-sectional shape that can be used to reduce drag is the so-called "streamlined" shape, which has a round or slightly elliptical leading edge and a gently tapering rear. This shape helps to minimize the amount of turbulence created as air flows over the surface of the aircraft, which in turn reduces drag and improves overall aerodynamic efficiency.

Another one that can be used to improve aerodynamic performance is the "wedge" shape, which has a sharp, pointed leading edge and a flat rear. This shape can be used to create a "shock wave" that helps to compress the air in front of the aircraft, which can increase the speed at which the aircraft can travel without generating excessive amounts of drag. It is not our case.

It is important to note that the cross-section shape is not the only aspect of aerodynamic design and it is often combined with other features such as wing design and placement, as well as the use of flaps and other high-lift devices [23], to achieve the desired performance characteristics of an aircraft.

There are some remarks to take into account when designing the external shape while using a cylindrical mid-section [18]:

- A frequently used value for the length/ diameter ratio is 1.5 to 2.0. A lower value may be used on freighters provided that this lightens the door and door support structure to such an extent that it outweighs the extra drag. This ratio is called the fineness ratio.

In our case, we will add to the height of the cabin the value of 0.23 m which is the result dimension for the fuselage and wing assembly. So, the total height is 2.2 m. Also, in terms of the width of the cabin, a margin will be added (0.14 m), so, the cabin's width will be 1.84 m. However, the diameter varies depending on the section; the fineness ratio of the tubular part of the ONA Jet fuselage is 2.73.

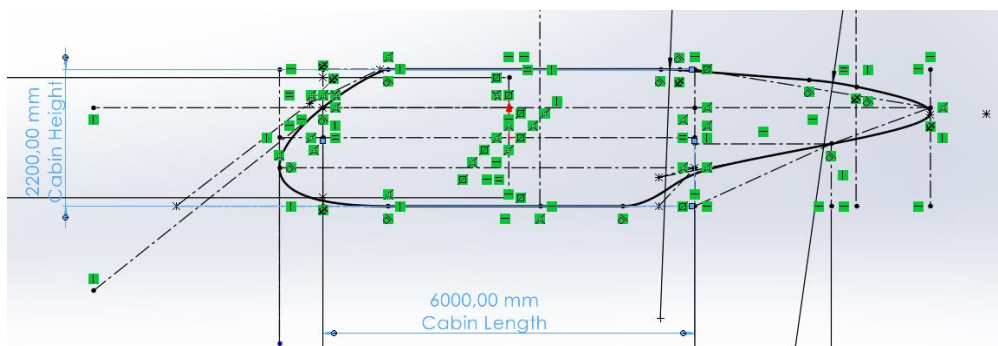


Fig.3.10 Fineness ratio dimensions

- All passenger transports and many highspeed general aviation aircraft have a radar installation, for which a reflector must be planned in the nose section.
- On small aircraft the fuselage nose can be used to contain Nav/Com equipment and/or luggage. In our case, the ONA Jet will carry the avionics compartment in the fuselage nose.

Regarding the tail section there are also some remarks to follow when there is a non-cylindrical rear part. There is not cylindrical because for the HEMS (figure 3.11) and SAR configurations, we need to place the tail in the upper part of the fuselage. It is because an access door will be placed in the back for these kind of operations in order to use the equipment they need according to the operation. A lateral door would be studied in a future for this kind of operations taking into account the possibility to pressurize when closed.

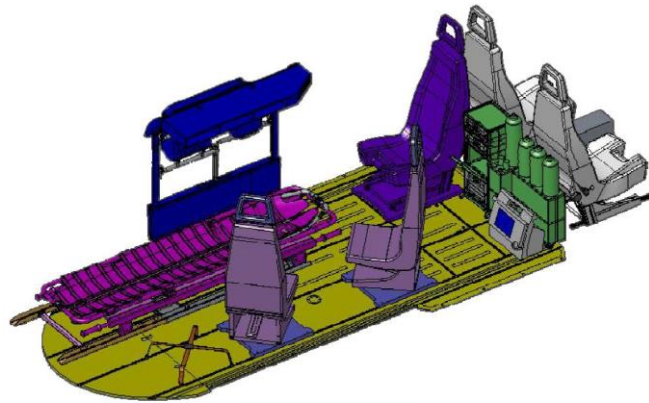


Fig.3.11 HEMS cabin configuration designed in 3D

So, the remarks for designing the rear part of the fuselage are:

- To avoid large regions of boundary layer separation and the associated drag increments, the tail length is usually 2.5 to 3 times the diameter of the cylindrical section, remarking that the diameter will be the cabin high plus the wing maximum thickness, thus a diameter of 2 meters.

However, in our case we are dealing with a relatively small aircraft, so, the fuselage tail length is determined by the tailplane moment arm required [24]. A reasonable value for the distance between the wing and horizontal tailplane quarter chord points is 2.5 to 3 times the wing MAC [23].

Even though the factor between 2.5 and 3 is a reasonable value, according to the V-Tail study [24] there's the need of applying a factor of 3.43, then (figure 3.12):

$$\text{Distance CG to } 1/4 \text{ chord } V - \text{Tail} = 1.2 \times 3.43 = 4.11 \text{ meters} \quad (3.4)$$

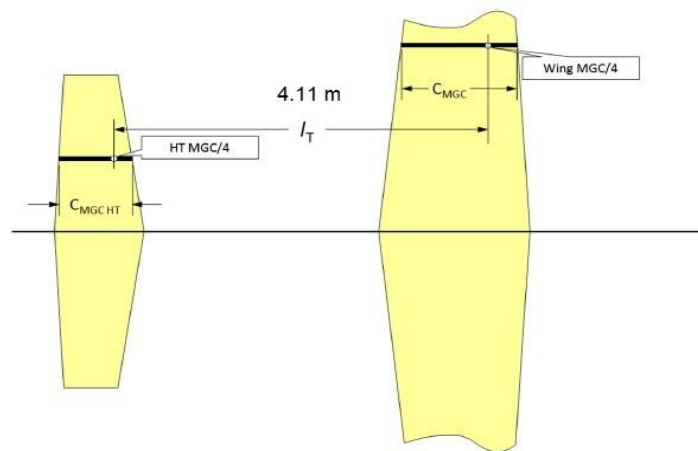


Fig.3.12 Distance between V-tail and wing MGC/4 [12]

- For ease of production, part of the fuselage tail may be conical; half the top angle of this cone should be 10° to 11° , or at most 12° . The transition between the cone and the cylinder ought to be smooth with sufficiently large radius of curvature.
- Tail cross-sections may approximate circles or standing ellipses in shape. Beaver tails have unfavorable drag characteristics and should be avoided on civil aircraft.

Regarding our tail, the Cambered fuselage tail is applied. The rear part of the fuselage is often slightly upswept in order to obtain the required rotation angle during takeoff or landing. The drag resulting from this slight camber is negligible. However, on freight aircraft with a rear loading door, which is our case, the fuselage must be swept up over a considerable angle, especially on small freighters like the De Havilland Caribou and Buffalo [32].

Adverse interference may occur in the flow fields induced by the wing (downwash), the wheel fairings and the rear fuselage. The formation of vortices below the rear part of the fuselage is shown in figure 3.12. These vortices are unstable and can cause lateral oscillation, especially at low speeds, high power, and high flap deflection angles. A considerable drag penalty in cruising flight is also caused by a large fuselage camber. Sharp corners on the lower part of the fuselage may relieve the problem by generating stable vortices, inducing upwash below the fuselage and thereby creating attached flow.

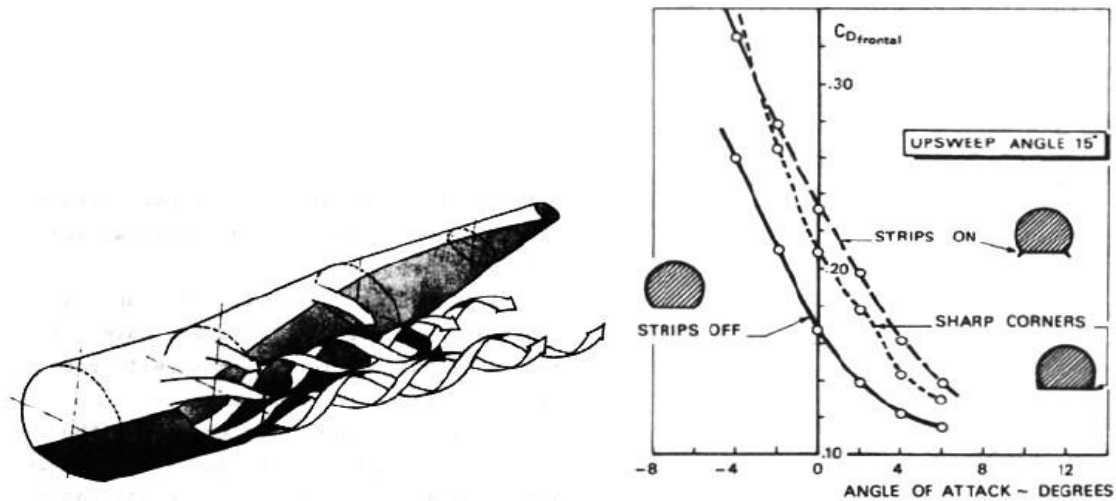


Fig.3.12 Formation of vortices below the rear part of the fuselage and sharp corners [18]

After defining the external dimensions, we must define the CG of the aircraft [26]. It is important because the center of gravity is the point over which the aircraft would balance and it ensures the stability of the aircraft.

In order to calculate the CG, we must follow the following steps:

- Determine the weights and arms of all mass within the aircraft.
- Multiply weights by arms for all mass to calculate moments.
- Add the moments of all mass together.
- Divide the total moment by the total mass of the aircraft to give an overall arm.

As the ONA Jet is in an early preliminary design (figure 1.2), we can't determine the exact location of CG due to the lack of information regarding weights and loads, principally from engines and batteries. Furthermore, depending on the configuration the CG could slightly vary but could be fixed by applying the mass and balance. This procedure will be implemented in the ONA Jet's future AFM (Aircraft Flight Manual).

In our case, in order to continue with the study, the CG is placed at $\frac{1}{4}$ of the MAC of the wing, in the figure 3.13 it is shown the preview:

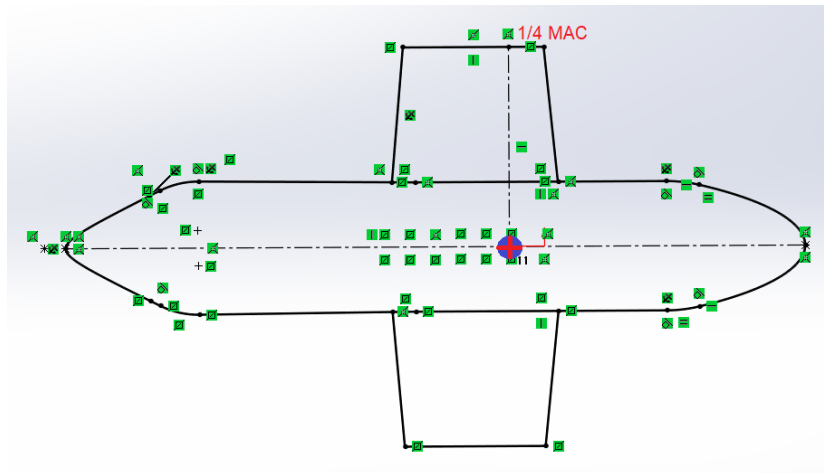


Fig.3.13 Preview of the CG in ONA Jet

3.5. Flight deck design (Visibility)

The ONA Jet will be able to perform flights in VFR (Visual Flight Rules) and IFR (Instrumental Flight Rules) conditions. When flying in VFR the pilot must have a clear view of such a part of the air space that he has adequate information to control the flight path and avoid collisions with other aircraft or obstacles. For design purposes this general requirement can be evaluated in the form of minimum angles of vision during cruising flight, takeoff, landing and taxiing.

When designing the nose of the aircraft there is some recommendation to take into account in order to respect the pilot's field of view and performing VFR flights without any problem. These are shown in figure 3.14.

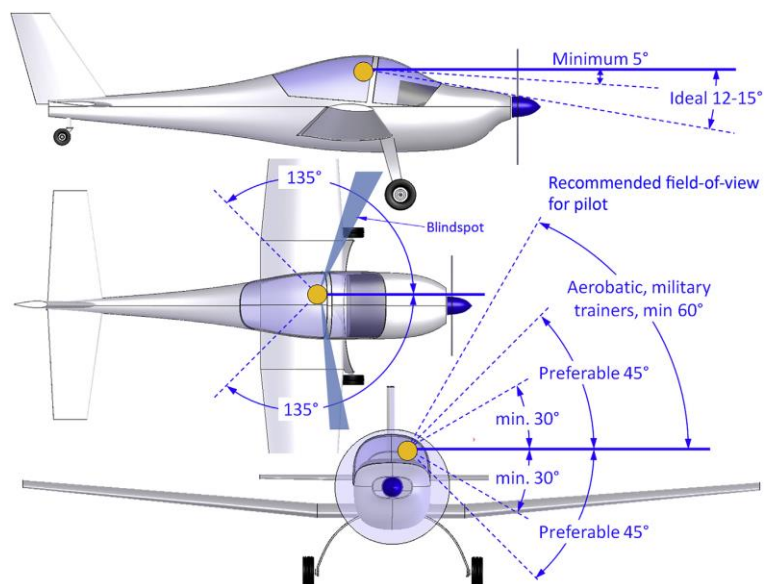


Fig.3.14 Pilot's field of view [12]

Basically, in the front view the pilots must have at least 5° of visibility from the horizontal axis, ideally $12-15^\circ$. What concerns the lateral views, it should respect in the horizontal view a minimum of 135° for each side from the central axis of the aircraft; and in the vertical view, a minimum of 30° up and down, preferably 45° .

Chapter 4. Methodology

In this chapter it is explained the two main software used to carry out the simulations.

4.1 SolidWorks

SolidWorks [11] is a comprehensive 3D modeling software that covers the entire product development process from design to simulation and documentation. It provides a wide range of tools for creating, editing and optimizing complex parts, assemblies and product drawings. SolidWorks also provides simulation tools, such as finite element analysis (FEA) and computational fluid dynamics (CFD), which allows to test and validate product designs before actual production. It also provides tools for creating technical illustrations, animations, and visualizations of the product, making it easier to communicate design concepts to stakeholders and customers.

On this project, SolidWorks is mainly used for designing the fuselage with the dimensions previously defined in chapter 3 and thus, having a 3D view of the body fuselage. It is also used to create the fluid domain in 2D for the simulations carried out in Ansys Fluent.

4.2 Ansys

Ansys [10] is a comprehensive simulation software that provides a platform to perform virtual testing and validation of product designs. The software integrates with CAD tools and offers a suite of simulation tools that enables to analyze and optimize product designs in a virtual environment. This helps to reduce the time and cost associated with physical testing and prototyping, and to improve the overall quality of the final product.

ANSYS provides a range of simulation capabilities, including FEA, CFD, multi-physics simulation, and optimization. FEA allows to analyze the structural mechanics of a product, such as stress, strain, and deformation, while CFD helps to predict fluid flow, heat transfer, and other fluid dynamics-related problems, which is the case of this project.

Now, the turbulence model and mesh are tackled. Regarding the turbulence model [34], Ansys offers different scale-resolving simulation (SRS) models (SAS, DES, SDES...).

The models typically require special attention to various details such as: model selection, grid generation (mesh), numerical settings, solution interpretation, post-processing and quality assurance.

Regarding the model selection, the SST K- ω turbulence hybrid model (DES: Detached Eddy Simulation) was selected. To solve the simulation, it combines the benefits of both K- ϵ and K- ω turbulence models. The K- ϵ model (LES: Large

Eddy Simulation) is used for inlet and free stream to avoid errors from the sensitive K- ω model, but the SST switches back to K- ω (RANS: Reynolds-Averaged Navier-Stokes) near the boundary layer due to its good behavior in adverse pressure gradients and flow separations. This model is widely used in the aerospace industry for its time-efficiency, precision, and recommendation for jet streams CFD simulations [34]. The inlet, outlet, and airfoil regions were defined after choosing the turbulence model: the studied region was set as the boundaries forming the airfoil/wing shape, the inlet region was set as the front, upper, and lower boundaries to account for rotational air flow, and the outlet region was set as the right-most boundaries of the field. All these criteria are shown in chapter 6.

In the simulation process it is important to mention as well the two main concepts used to define the mesh and ensure its quality, these are the inflation and the meshing metrics.

Regarding the wall conditions, the thickness of the inflation layer applied at the body is determined by a dimensionless parameter called y^+ . This parameter is utilized to guarantee that the turbulence model selected accurately predicts the fluid's behavior near the airfoil's wall in boundary layers with unfavorable pressure gradients. As smaller is the y^+ value, more accurate will be the prediction. For all models except LES, use low y^+ values of around $y^+=1$. As it is used DES, this value must be smaller than 1. The flight parameters are introduced in the referenced tool [33] and it is obtained a $y^+= 1 e-5 m$.

Once the inflation parameters are defined it is used the equation 4.1 to check if the inflation tool satisfies the y^+ condition in order to obtain a mesh with a good quality.

$$1st\ Layer\ Thickness = \frac{Max\ Thickness \cdot (1-g)}{1-g^{N+1}} \quad (4.1)$$

Where N is the number of layers set up and g is the growth rate.

Regarding the meshing metrics, these are numerical values that describe the quality and characteristics of a mesh, which is a collection of interconnected points, lines, or surfaces used to represent a complex geometric shape in computer simulations. For the study it is taken into account the following metrics (figure 6.10):

- **Element Quality:** This metric describes the quality of individual elements in the mesh, such as triangles, quadrilaterals, or hexahedrons. The quality of an element is determined by its shape, size, and aspect ratio, and is an important factor in the accuracy and stability of numerical simulations. In the studied mesh it is chosen the triangles (figure 6.6).
- **Element Count:** The number of elements in a mesh is an important factor in determining the computational cost of a simulation. A high element count can lead to increased computational time and memory

requirements, while a low element count can result in a less accurate representation of the geometry. The number of elements is 500971 (figure 6.9).

- **Maximum and Minimum Element Size:** These metrics describe the range of element sizes in a mesh, which is an important factor in determining the resolution of the simulation. A mesh with a small maximum element size will provide a more detailed representation of the geometry, while a mesh with a large maximum element size will result in a coarser representation.
- **Non-Orthogonality:** This metric describes the degree to which elements in a mesh deviate from a perfect 90-degree angle. A mesh with high non-orthogonality can result in reduced accuracy and stability in numerical simulations. It is set up 30° .
- **Skewness:** This metric describes the degree to which elements in a mesh are distorted, which can result in reduced accuracy and stability in numerical simulations.
- **Aspect Ratio:** This metric describes the ratio of the longest side of an element to the shortest side, which is an important factor in determining the quality of an element. A high aspect ratio can result in a distorted element, which can impact the accuracy of a simulation.

Last but not less important the convergence criteria. For the ITA (iterative) schemes, the segregated solvers are typically faster than the coupled solver. For SRS model simulations, they should be changed to values as close as possible to 1 to improve iterative convergence. The most critical quantity is the mass conservation. Mass residuals and static pressure should decrease by at least one order of magnitude every time step. With high under-relaxation and good grid quality, good solutions can often be achieved even with only two inner loops. Simply residuals are a function of the error in the model. The higher the residual the less good the solution. Note, it could be obtained fairly high residuals due to local effects but overall had a decent solution.

In the case of this study, it is set up a stop criterion of $1e-8$. I.e., when the static pressure values between the current and the previous iteration differs a number smaller than the stop criterion will mean that it converges and will stop. Otherwise, it will keep iterating.

Chapter 5. Body Design

Once the ONA Jet concept has passed through the points defined in chapter 3 and taking into account the requirements shown in table 3.1, we can start defining the body. Initially was tried to look for a configuration such as Tadpole, but our tail is cambered and cannot be done.

However, the type of fuselage which could fit with the ONA Jet concept is the Pressure Tube Fuselage, i.e., the classical commercial fuselage.

First, it is drawn in SolidWorks [11] the lateral view of the dimensions which were designed but adding some remarks and modification due to the selected configuration (figure 5.1):

- **Cabin length:** 6 m + 0.7 m for cockpit layout. This cockpit layout is necessary for the installation of radar, COMs and, principally, avionics among others.
- **Cabin height:** 2.2 m.
- **Distance between Wing and V-Tail:** In the preliminary design, initially this distance was 4.11 m. However, in the measurements was not taken into account the rear eDFAN of the ONA Jet, so, this distance is no more valid. The eDFAN is expected to have a diameter of 2.2 m. Thus, after redesigning the tail we arrived to the conclusion that the distance, for a total length of 10.5 m, should be at least 5.1 m.
- **Degrees of visibility:** In terms of the visibility, we needed around 15° . As the ONA Jet nose is not so flat, we achieve with the current design a visibility of 38.48° .

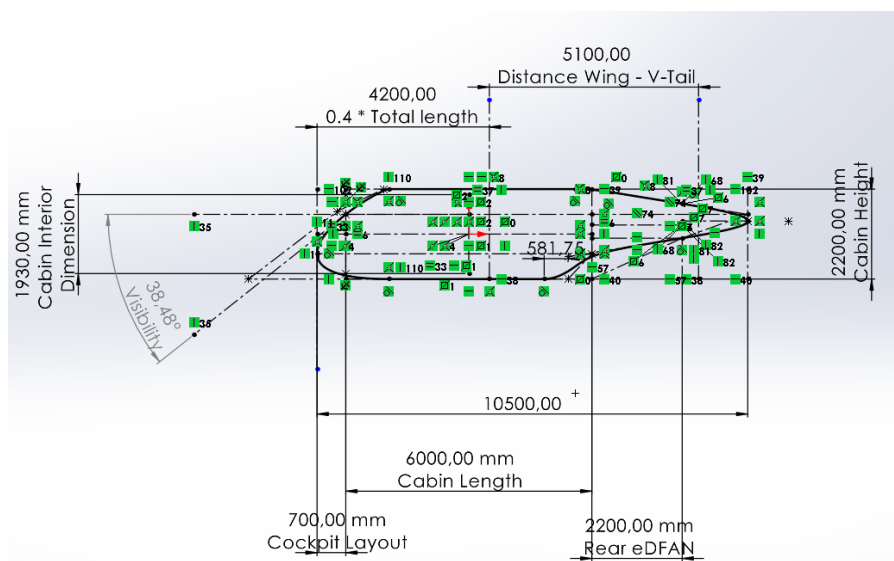


Fig.5.1 Body lateral view dimensions

In figure 5.2 it is defined as well the dimensions of the plan view.

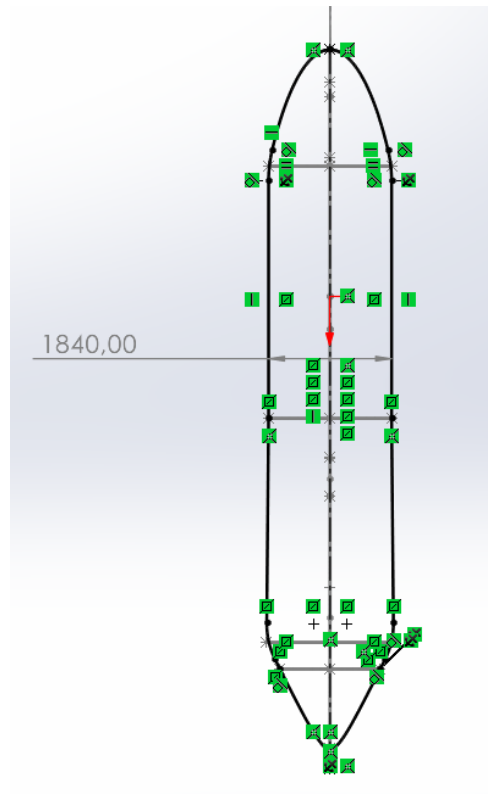


Fig.5.2 Body plan view dimensions

Secondly, in order to obtain a 3D concept of the fuselage we will draw the dimensions of the frontal section. We will follow the same procedure, drawing the dimensions and applying relations until the drawing is completely defined.

The dimensions will not be the same through the entire fuselage, even though the cabin height is already taking into account in the lateral view, we will define the diameters in the crucial points such as in the nose and in the tail where the V-Tail is placed. As an elliptical cross-section is implemented in the tail, we will establish, together with the V-Tail study [24], the “horizontal diameter” or width. Then, these sections are defined:

- **Cabin Cross Section:** Circular/ Elliptical
- **Cabin Width at the mid-cross Section:** 1.84 m
- **Tail width at 5.1 m from CG:** 1.5 m

In order to define these sections, different planes will be created different planes at the desired distances such as shown in figure 5.3.

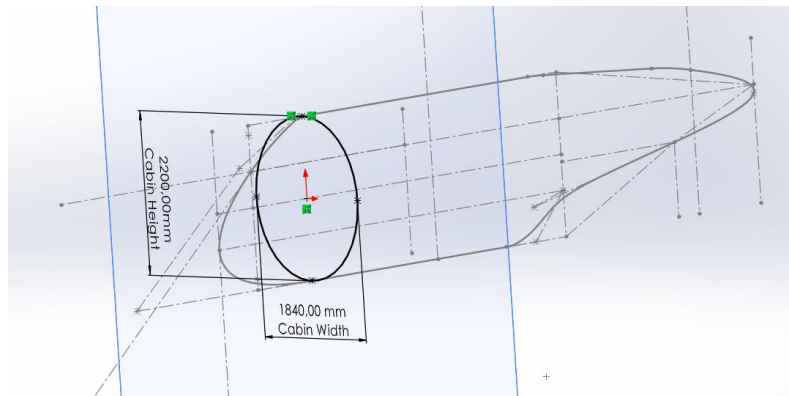


Fig.5.3 Early body frontal view dimensions

Once the cross shapes are defined, it is obtained the fuselage plan. (Figure 5.4)

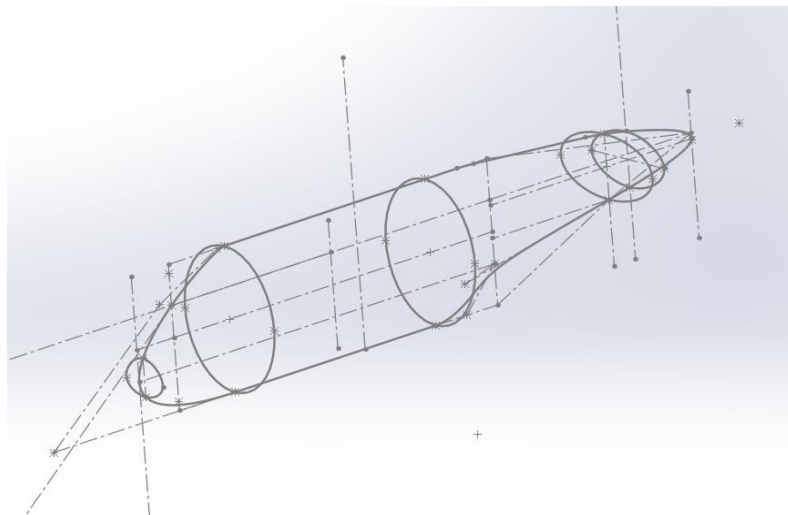


Fig.5.4 Fuselage plan

Then, in order to obtain the body in 3D, the cross section should be extruded along the longitudinal shape.

This procedure will consist in dividing the longitudinal shape of the aircraft in two: the upper part and the lower part. This operation is carried out through the operation “trim identities” and selecting the shape we are interested in.

It is also needed to split in two parts the plan view shape (figure 5.2): left and right. However, since the fuselage is not a perfect cylinder through the longitudinal axis, it is needed to do the procedure for the longitudinal axis of each cross-section, i.e., there will be a left and right sections for low, mid and high level. These ones will act as guides for the coating tool. Low level deals with the nose cross-section, mid-level deals with the mid cross-section and

high-level deals with the tail cross-section. The result is shown in figure 5.5. The different blue lines are the different guide split sections.

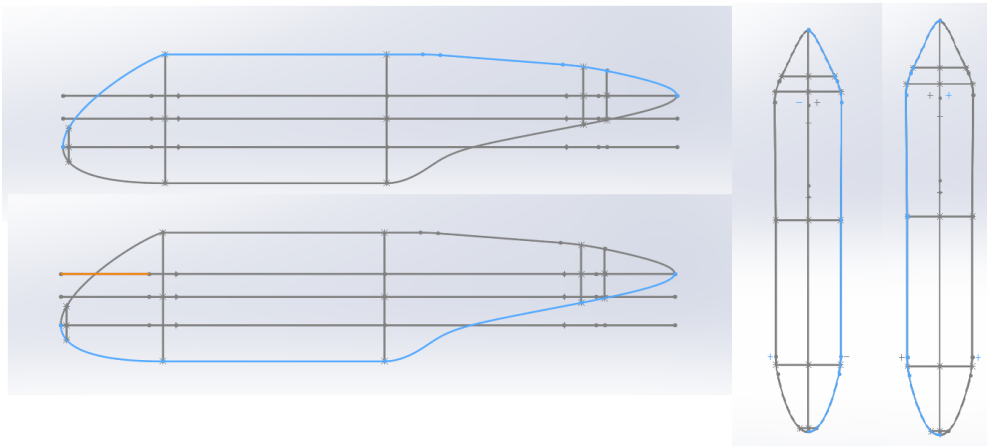


Fig.5.5 Split fuselage

The idea is to avoid sharp corners rounding these ones because it would cause turbulence and separation of flow, leading to increased drag and decreased aerodynamic efficiency. The separation of flow can also lead to flow detachment, creating a region of low pressure that generates even more drag.

Now, it is applied coatings using the different cross-sections and the guides created by splitting the fuselage. (Figure 5.6)

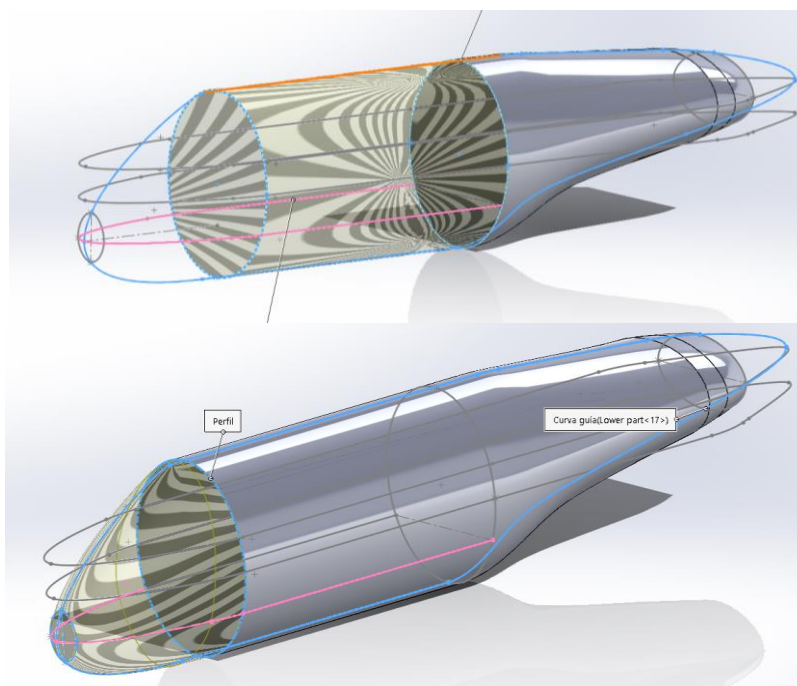


Fig.5.6 Coating the fuselage

Finally, the body fuselage is obtained, it is shown in figure 5.7 painted in white. The ONA Jet will be painted in this color for the reasons below:

- Less damage from solar radiation because this color has the most albedo.
- Passengers and crew stay cool and comfortable.
- Easier to spot damage.
- Reduce the chances of bird strikes.
- White doesn't fade like darker colors.

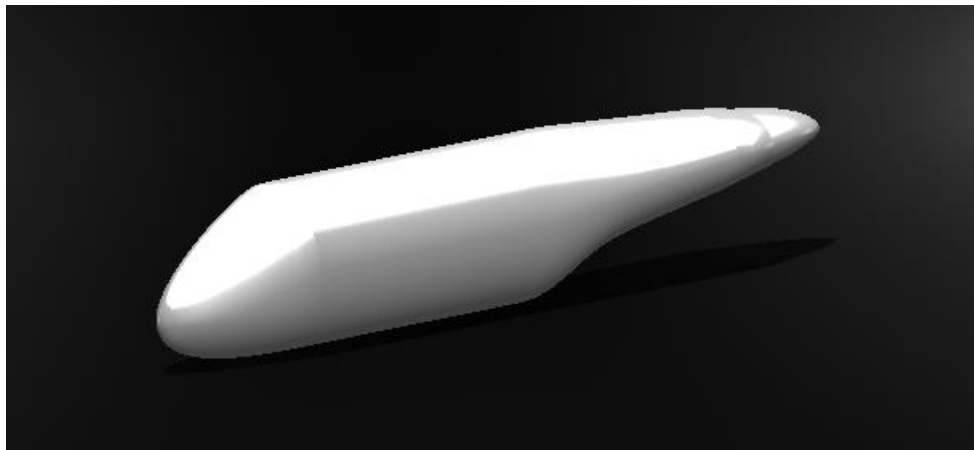


Fig.5.7 Body fuselage painted in white

Chapter 6. Body aerodynamic study

This chapter deals with the aerodynamic study of the body fuselage in cruise conditions. It is carried out using Ansys Fluent with a student license. It means a limitation in terms of computing number of cells. In order to simulate the body fuselage with a minimum accuracy, the numbers of cells needed for 3D is around 1 million cells. The student license is limited to 512000 cells.

Then, due to the number of cells limitation, the study is carried out considering the body fuselage profile, i.e., in 2D. Thus, the body fuselage is considered as an airfoil profile (shown in figure 5.1) for the simulation.

Simulating an airfoil profile in 2D is interesting because it allows for a relatively simple and computationally efficient way to study the basic principles of aerodynamics. By modeling an airfoil in two dimensions it could be observed the behavior of the airflow over the surface and analyze the resulting lift and drag forces. This can provide valuable insights into the design and performance of body shape.

Two-dimensional simulations are particularly useful for understanding the flow patterns and pressure distributions that are present in real-world scenarios, and for optimizing the shape of an airfoil for a specific purpose, as it shown throughout this chapter.

The aim of this study is to obtain the aerodynamic properties of the current body fuselage shape and knowing if it satisfies the proposed requirements, which principally is achieving the generation of the 25% of the total lift.

Furthermore, if this requirement is not achieved, it is needed to have in mind that the ONA Jet is still in the preliminary design, so, any information received from this study will serve as hints in order to know if we are in the right direction.

First, the fluid domain is designed in SolidWorks [\[11\]](#).

To do this, the first that is needed to define is the optimum domain for 2D. This means a circular shape in the front and a rectangular shape in the rear. It is done in this way because when simulating for different AoAs the entering wind will have the same distance to the leading edge (Aircraft's nose) since it is a circle and its radius is constant. It will enable the study to save grid cells which do not improve accuracy.

There is, principally, two dimensions to define the fluid domain. It is recommended to take these limits at five times the chord of the body (10.54 m) for the upper, lower and front side. Then, taking ten times the chord for the rear side.

So, our dimensions will be:

$$\text{Dist. Front, Top and Bot} = \text{Body Chord} * 5 = 10.54 * 5 = 52.7 \text{ m} \quad (6.1)$$

$$\text{Dist. rear limit} = \text{Body Chord} * 10 = 10.54 * 10 = 105.4 \text{ m} \quad (6.2)$$

After applying the distances to the fluid domain drawing, in figure 6.1 is shown the result.

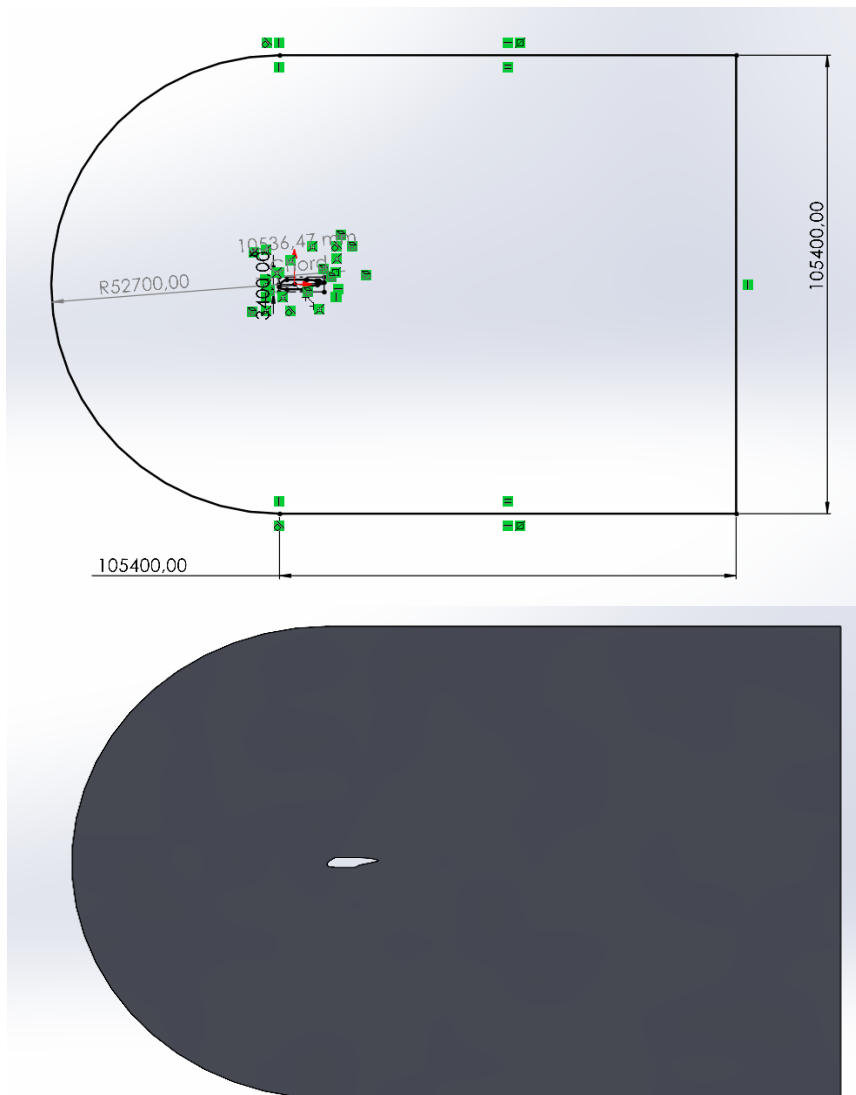


Fig.6.1 Drawing of the fluid domain

Once the fluid domain is defined, it is used the Ansys Fluent [10] in order to simulate the body profile in flight conditions. Then, it is needed to set up the Ansys Fluent parameters (Fig. 6.2).

First, the body fluid domain it is imported at the design modeler. Once it is loaded, we select the part and then at the left lower corner there is the menu where we can fix the parameters (Fig. 6.3). At this point, the part is defined as fluid.

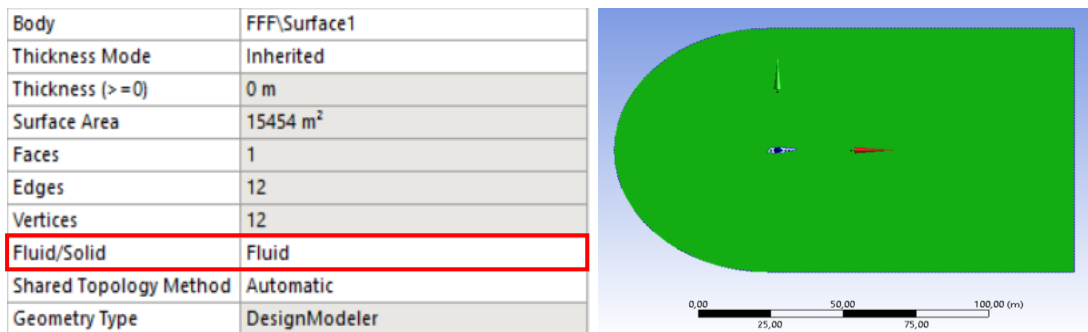


Fig.6.3 Fluid definition

The following step is applying a rotation since the idea is to simulate the body profile for different angles of attack. Then, inside the tool create body transformation we select rotate. At the same place than before, left lower corner, we set up the angle parameters (Fig. 6.4): initial angle of attack and the axis at which the profile will rotate, in our case the XY axis.

Details of Rotate1	
Rotate	Rotate1
Preserve Bodies?	No
Bodies	1
Axis Definition	Selection
Axis Selection	Plane Normal
P FD9, Angle	0°

Fig.6.4 Angle of Attack definition

Once the fluid and the AoA are defined, we proceed to generating the mesh. First, it is defined the inlet, outlet and body. It is done by selecting the edges for each name selection by right-clicking and assigning it to the inlet, outlet or body. Once it is done, we could see the different name selections being A: Inlet, B: Outlet and C: Body. (Fig. 6.5). It is important to remark that the inlet is not just the semi-circle but also the top and bottom of the fluid domain part.

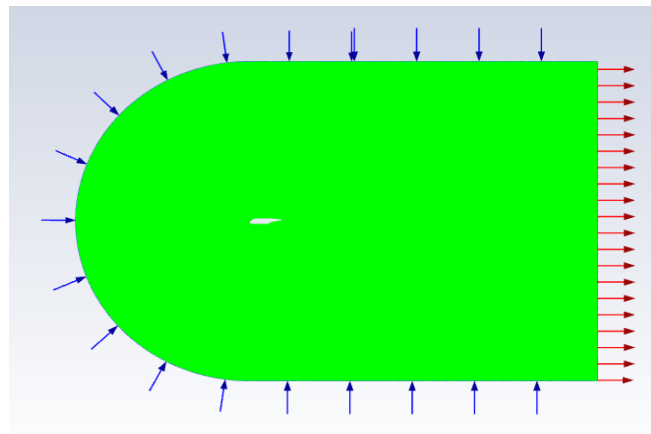
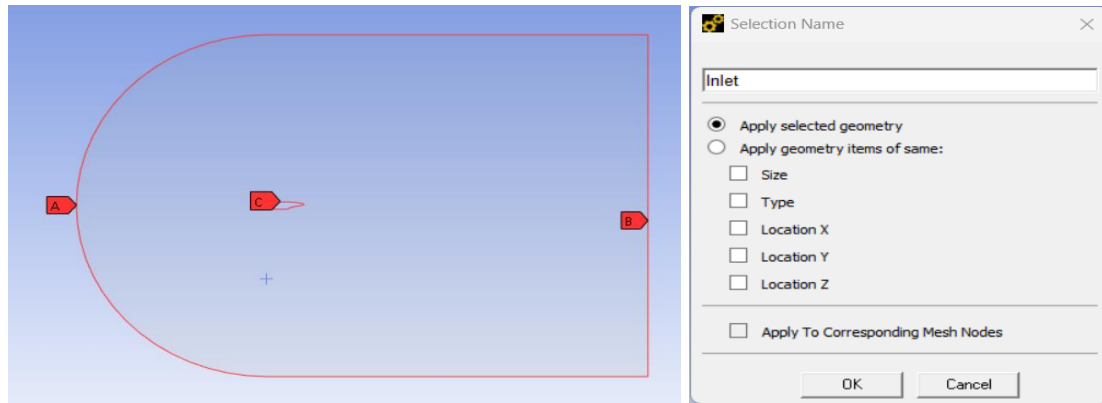


Fig.6.5 Inlet, Outlet and Body definition

The next step to follow is creating the mesh. Right-clicking the mesh it is selected the option “Method”. At this point we select the part and apply as method the triangles one (Fig. 6.6). There is also quadrilateral and a mix of them, but it is chosen triangles because it is obtained almost the same results as the quadrilateral with a smaller number of cells. As the student version is limited in terms of cells, the space optimization is a must.

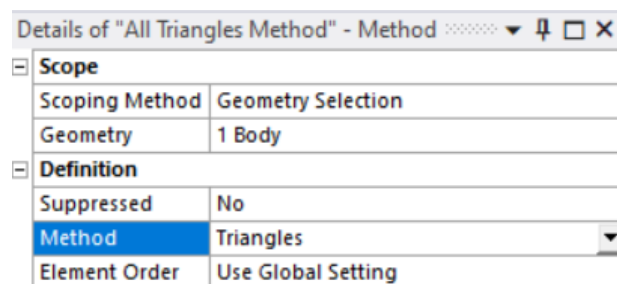


Fig.6.6 Method details

After, the tool sizing is inserted to the mesh. To do so the body profile edges are selected and this tool is applied. Then we fix the parameters on the menu by setting the number of divisions to 310 (Fig. 6.7).

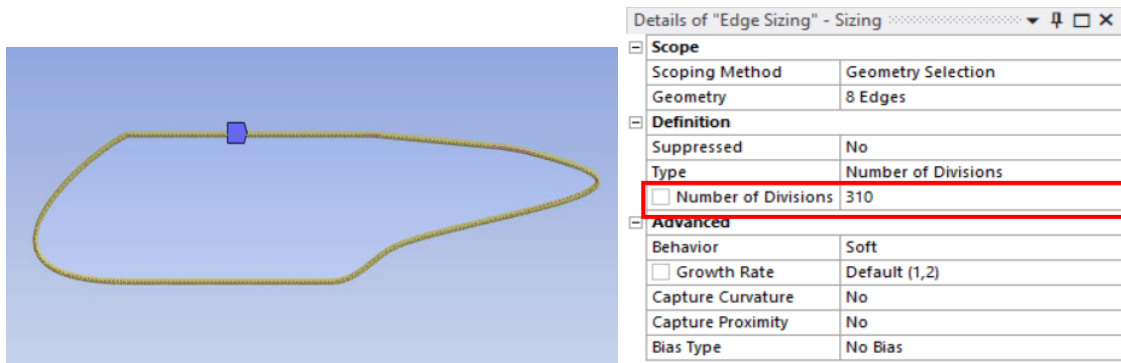


Fig.6.7 Sizing parameters

The last step to finish with the mesh is applying the inflation tool. This tool creates a region near the body profile edges where the cells are smaller than the other ones in order to gain resolution on this zone and increase the accuracy of the results by providing a better capture of the fluid's behavior surrounding the airfoil.

Scope	
Scoping Method	Geometry Selection
Geometry	1 Face
Definition	
Suppressed	No
Boundary Scoping Method	Geometry Selection
Boundary	8 Edges
Inflation Option	Total Thickness
<input type="checkbox"/> Number of Layers	14
<input type="checkbox"/> Growth Rate	1,2
<input type="checkbox"/> Maximum Thickness	6,e-004 m
Inflation Algorithm	Pre

Fig.6.8 Inflation parameters

It is observed in figure 6.8 that it is chosen 14 layers with a maximum thickness of 0.0006 m. So, the first layer thickness for the chosen parameters is 8.33×10^{-6} which satisfies the $y^+ < 1$ condition and, also, $8.33 \times 10^{-6} < 1 \times 10^{-5} \text{ m}$ which is $y^+ = 1$ the most restrictive case.

Once the profile contours are defined and it is already applied the sizing and inflation methods, we can start generating the mesh and defining its parameters. (Fig. 6.9)

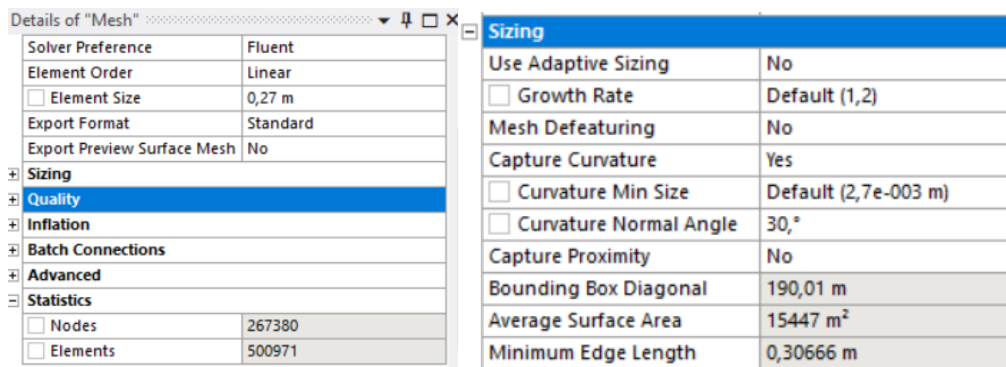


Fig.6.9 Details of Mesh and Sizing

In this case it is modified the element size, as smaller it is the parameters more elements will be and more time and computational cost will be needed. However, with a smaller element size it is achieved better results since there are more elements, also considered as a kind of resolution. In our case this parameter is set up at 0.27 m.

Then, inside the sizing parameters the mesh defeaturing is set up as "No" since it would simply the mesh and we are not interested in doing it. Also, it is needed to set up the curvature normal angle at 30°. It makes the mesh to adapt itself to the body. Finally, inside quality, the smoothing is set up at "High".

These are the meshing metrics explained in chapter 4.2 (figure 6.10).

Mesh Metric	Skewness	Mesh Metric	Element Quality
<input type="checkbox"/> Min	1,3058e-010	<input type="checkbox"/> Min	1,8681e-002
<input type="checkbox"/> Max	0,77541	<input type="checkbox"/> Max	1,
<input type="checkbox"/> Average	5,2193e-002	<input type="checkbox"/> Average	0,91862
<input type="checkbox"/> Standard Deviation	5,9865e-002	<input type="checkbox"/> Standard Deviation	0,19231
Mesh Metric	Aspect Ratio	Mesh Metric	Orthogonal Quality
<input type="checkbox"/> Min	1,	<input type="checkbox"/> Min	0,46023
<input type="checkbox"/> Max	104,08	<input type="checkbox"/> Max	1,
<input type="checkbox"/> Average	2,6967	<input type="checkbox"/> Average	0,96807
<input type="checkbox"/> Standard Deviation	8,2416	<input type="checkbox"/> Standard Deviation	3,7261e-002

Fig.6.10 Meshing metrics

It is important to remark that these parameters are adapted to the cell's limitations imposed by the student version, it is shown in figure 6.9 the number of elements, also known as cells, which is 500971. Always keeping in mind, a number of cells below 512000.

As a result, it is obtained the mesh shown in Fig. 6.11.

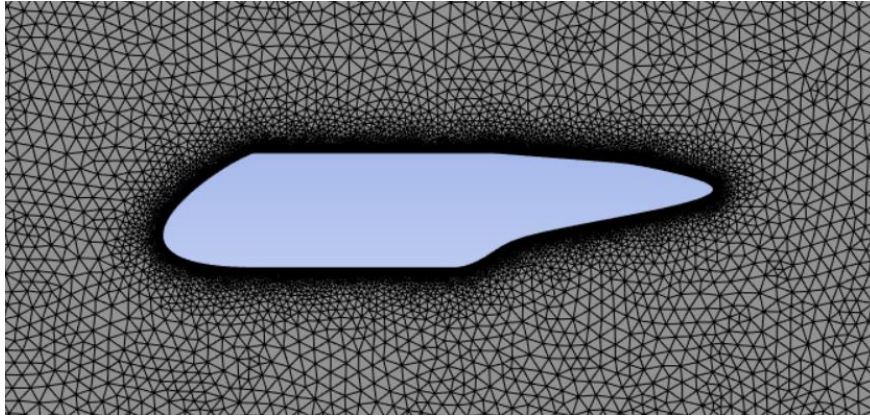


Fig.6.11 Mesh of the body profile zoomed

Once the mesh is created, it is proceeded to insert the flight parameters at the solution tab as well as defining the outputs we are interested in, i.e., the coefficient lift and drag for the different angles of attack.

Inside the results it could be obtained the plots of pressure distribution and streamline figure.6.12, for example.

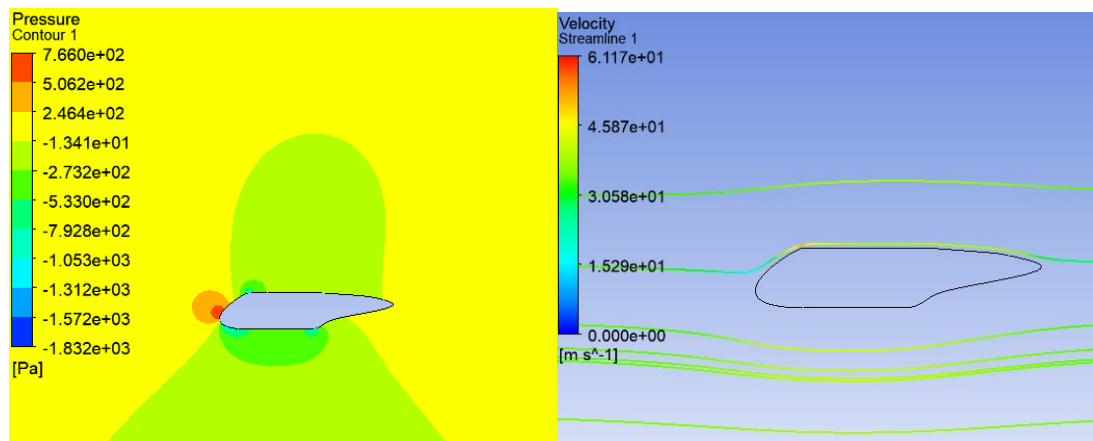


Fig.6.12 Plot of the pressure distribution and the streamlines at AoA = 0°

The last step to obtain the values we are interested in is updating the project and clicking the tab parameter where we can obtain the Cl and Cd for the AoA we input.

Normally the AoA in cruise is between 0° and 4°, being 4° a very optimistic angle of attack. Until the aerodynamic department establish the cruise AoA, the simulations are carried out by using the degrees inside this interval: 0°, 1°, 2°, 3° and 4°.

It is shown in the table 6.1. the evolution of the Cl and Cd with respect to the angle of attack. Since the simulation it is carried out using little AOA, the

variations of C_l and C_d are small but no negligible. All the C_l and C_d values are based on the chord of body fuselage shape.

Table 6.1. Aerodynamic properties for the ONA Jet fuselage (Version 1)

AoA	C_l Body	C_d Body	Efficiency (C_l/C_d)
0	-2.5947	0.1664	-15.5931
1	-1.7587	0,1508	-11.6702
2	-0.6583	0.1481	-4,4571
3	0.2931	0.1452	2,0716
4	1.1882	0.1382	8,5716

Regarding the C_l , it increases such as the AoA. So, the Efficiency does. In addition, the C_d decreases.

It is not that strange since usually the C_d , for small AoA, decreases as the C_l increases. This reduction could be caused by the shape of the cambered tail. I.e., at the belly of the body there is one moment where the tail starts going up and causing an abrupt change of the shape; at this point the air boundary layer starts detaching and creating a zone where turbulences appear causing the drag. So, as the AoA increases, it delays the detachment of the boundary layer causing a smaller turbulence region at the tail and, then, reducing the C_d .

Simulating in 3D all the simulation parameters and results would change. For instance, in 3D it would appear unstable vortices which could cause lateral oscillation, especially at low speeds, high power, and high flap deflection angles, one solution to this would be applying sharp corners on the lower part of the fuselage since it may relieve the problem by generating stable vortices, inducing upwash below the fuselage and thereby creating attached flow.

The evolution before exposed is shown graphically in the plots below:

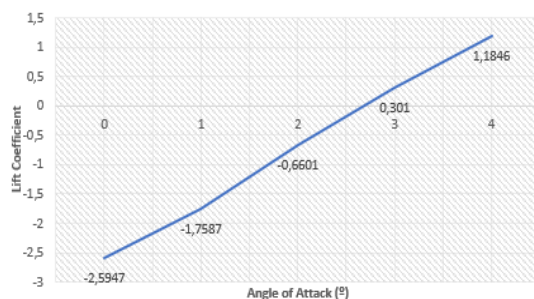


Fig.6.14 C_l vs AoA V1

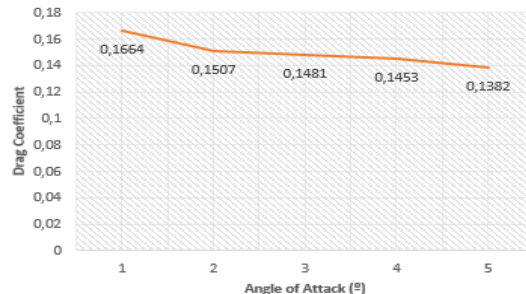


Fig.6.15 C_d vs AoA V1

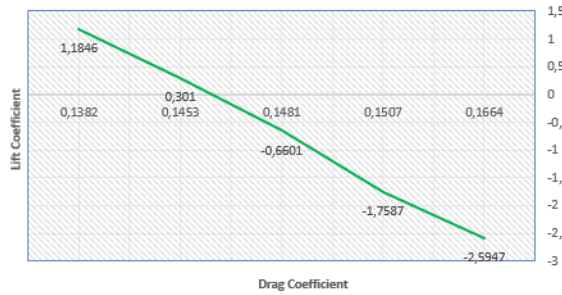


Fig.6.16 Cl vs Cd V1

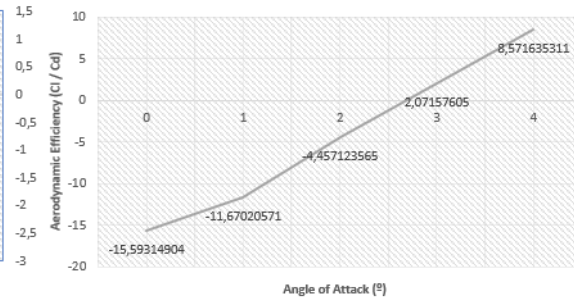


Fig.6.17 Cl/Cd vs AoA V1

Working together, the aerodynamic department of ONAerospace [23] [24] decided to fix the angle of attack, at cruise operations, at 3°. Then, we can compute the generated lift with the body profile using the equation (2.2) and the flight conditions shown in table 6.2:

$$L = \frac{1}{2} \rho v^2 S C_l = 3795.76 \text{ N} \quad (2.2)$$

Table 6.2. Flight conditions

Air density (k/m ³)	1.225
Speed (m/s)	35
Surface (m ²)	17.26
Cl	0.2931
Mass (Kg)	2950
Gravity (m/s ²)	9.81

Also, the cruise performance satisfies:

$$Lift = Weight = Mass * Gravity = 28940 \text{ N} \quad (6.3)$$

It is important to remark that the Cl and surface shown in table 6.3 are based on the chord of the body fuselage shape. The surface is extracted from the SolidWorks tool.

In order to verify if we achieved the percentage of the total lift required (25%), it is divided the Lift generated (2.2) by the Total Lift needed to satisfy the static analysis (6.3):

$$\% \text{Lift} = \text{Lift generated} / \text{Total Lift} * 100 = 13,12\% \quad (6.4)$$

The first version of the body shape didn't achieve the goal set at the beginning of the project. However, we can modify partially the body shape but keeping the interior dimensions, in order to gain more Cl and, then, producing more lift.

So, a **second version** of the body shape was designed:

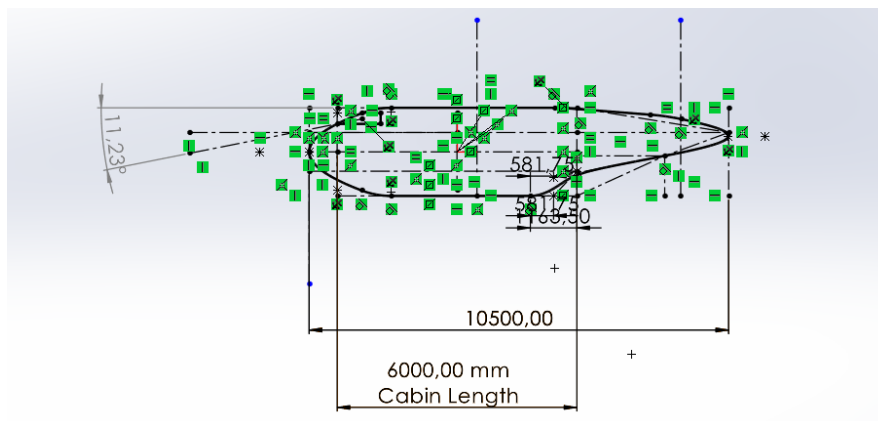


Fig.6.19 Body lateral view dimensions of the version 2

On this second version of the shape it is modified the nose of the body. It is placed the nose centered at the axis of the fuselage in order to make it more symmetrically at the leading edge.

However, the body kept its cambered shape since the rear part can not be modified. It is because of the main different configurations the ONA Jet is designed for.

On this new version the visibility is reduced considerably but still inside margins, the current visibility is 11.23°.

Regarding the chord, it remains almost the same, before was 10.54 m and now 10.51 m. It is slightly reduced since the nose of the aircraft (LE) is almost at the same level as the tail (TE), so the distance is a bit shorter.

In terms of defining the fluid domain, it is obtained almost the same results, since the chord is practically the same

$$\text{Dist. Front, Top and Bot} = \text{Body Chord} * 5 = 10.51 * 5 = 52.55 \text{ m} \quad (6.5)$$

$$\text{Dist. rear limit} = \text{Body Chord} * 10 = 10.51 * 10 = 105.1 \text{ m} \quad (6.6)$$

After defining the parameters on SolidWorks for the fluid domain and the other simulation parameters on Ansys as done for the body profile of version 1, the obtained the results for the version 2 are shown in table 6.3.

Table 6.3. Aerodynamic properties for the ONA Jet fuselage (Version 2)

AoA	Cl Body	Cd Body	Efficiency (Cl/Cd)
0	-2.1140	0.1630	-12.9693
1	-1.2382	0.1531	-8.0875
2	-0.3481	0.1459	-2.3859
3	0.6895	0.1422	4.8488
4	1.6150	0.1379	11.7114

On the one hand, before plotting the results, the first parameters which catches our attention is the Cl for all the angles since are bigger than before, to begin with it is a good sign. We will focus on the Cl value for 3° since it is the cruising AoA.

On the other hand, we observe the same evolution for the aerodynamic efficiency, increasing, and for the Cd, decreasing, when increasing the angle of attack.

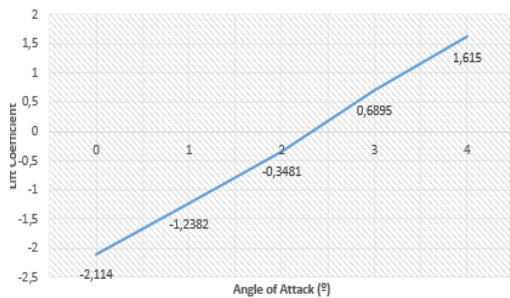


Fig.6.20 Cl vs AoA V2

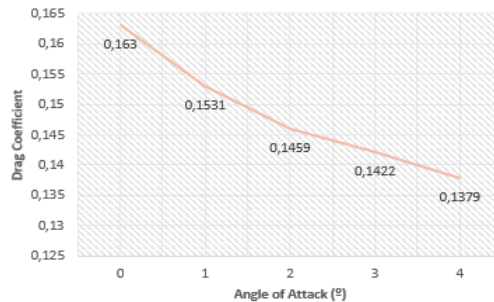


Fig.6.21 Cd vs AoA V2

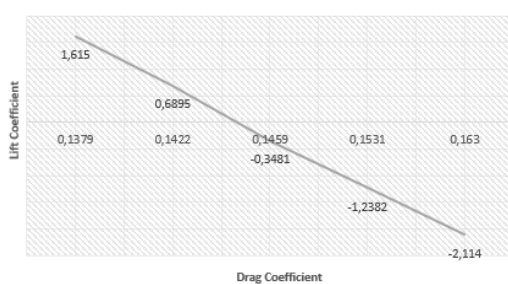


Fig.6.22 Cl vs Cd V2

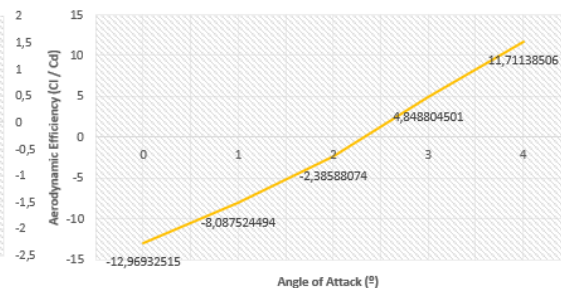


Fig.6.23 Cl/Cd vs AoA V2

Now, it is proceeded to compute the % of the total lift generated to ensure if at this version the goal is achieved for a $Cl(3^\circ) = 0.6895$. So, applying the equation 2.2 and 6.4 as done in version 1 but for the new Cl we obtain:

$$L = \frac{1}{2} \rho v^2 S C_l = 8929.30 \text{ N} \quad (2.2)$$

$$\% \text{ Lift} = \text{Lift generated} / \text{Total Lift} * 100 = 30.86\% \quad (6.4)$$

According to the simulations carried out in 2D, from the body version 2 it is obtained a 30.86% of the total lift. Initially it is an advantage because we achieve more lift than the one expected, however, in order to maintain the aircraft stability in the cruising performance the aircraft should have a load factor of 1 (equation 6.7), being the load factor, the lift divided by the weight.

$$n = L/W \quad (6.7)$$

Assuming that the wing study [23] and V-Tail study [24] generate 90% and -3% respectively, summing all the components it is obtained a load factor of:

$$n = 0.3086 + 0.9 - 0.03 = 1.1786 \quad (6.7)$$

In order to be in equilibrium, the load factor should be 1 and it could be fixed by applying this main three different options:

- Reducing the AoA in Cruise.
- Reducing the lift generated by the wings. For instance, reducing the span.
- Redefining the body shape in order to achieve less lift.

As mentioned at the beginning of this chapter, the simulations are not carried out in 3D because of the cell's limitations (512000 cells). Despite this, we obtained an approximation doing it in 2D. The need of 3D simulations is needed in further studies of the body fuselage because these main reasons:

- **Increased realism:** it provides a more accurate representation of the complex flow patterns and pressure distributions that are present in real-world aerodynamic systems. This can lead to more accurate predictions of aerodynamic performance and a better understanding of the underlying physical processes.

- **Improved representation of turbulence:** Turbulence is a complex and highly three-dimensional phenomenon. Simulating turbulence in three dimensions provides a more accurate representation of its behavior and a better understanding of its impact on aerodynamic performance.
- **Better representation of wing-body interactions:** In many aerodynamic systems, the flow around the wing is closely related to the flow around the body. Three-dimensional simulations allow for a more complete representation of these interactions, leading to a better understanding of the overall aerodynamic performance.
- **Improved representation of vortices:** Vortices are swirling patterns of air that can have a significant impact on aerodynamic performance. Three-dimensional simulations provide a more accurate representation of the formation and behavior of vortices, allowing for a better understanding of their impact on the aerodynamic system.

It would be interesting to carry out the simulation in 3D specially paying attention how the drag evolves, since it is the principal inconvenient of the body, and, therefore, computing the real aerodynamic efficiency of the current concept.

Conclusion

The airframe design solution achieved the goal initially proposed, generating minimum a 25% of the total lift required in cruise. The aiming of this study is designing the airframe concept to know if we are on the right way.

As the ONA Jet is in a conceptual and preliminary design, there is a lot of aspects to improve. In this study it is realized that on this phase of the project there is a lot of try and errors. I.e., on the first body version the airframe not even achieved a 20% of the total lift, in fact, was just a 13.12%. Then, it is redesigned the nose of the aircraft in order to change the aerodynamic but keeping some dimensions due to the internal space, the cabin. On this second version of the body, it is finally accomplished the 30.86% of the total lift. It has advantages and inconvenient depending on how it is used this extra lift. It is commented at the end of this conclusion regarding the further work.

It is imperative to have in mind that the study is carried out in 2D simulations. For obtaining realistic results the simulations must be carried out in 3D which will change all the results previously obtained.

As further work, it is interesting depending on the aircraft configuration, the fact that in case of pressurizing it would be needed to study the possibility of implementing a sliding door and the rear cargo door. Furthermore, as we are pressurizing the aircraft, there is also needed a study of the windows shape and structure.

It is important to keep in mind that the idea is to have a retractable landing gear since it produces less drag at the cruise. Then, it is interesting to tackled in future studies the space needed at the body fuselage for the retractable landing gear, specifically at the belly.

In terms of stability, we generate more lift than the one expected to equalize the weight which is good from a certain point of view. However, it means an unstability in the vertical axis but it could be fixed by applying these main three different options: reducing the AoA in Cruise, reducing the lift generated by the wings (reducing the span...) or redefining the body shape in order to achieve less lift.

It is difficult to find the optimal solution to this concept since there is a constantly of trade-offs, but not impossible. Some companies like Joby Aviation [7], Lillium [8] and Volocopter [9] are working on this concept as well. It is interesting to analyze how they arrived to the advanced phase of its projects and what are the error they committed in order to avoid them.

It is trusted that the ONA Jet will become true in the following years and that the ONAAerospace, with its UPC engineers' team, accomplish the aircraft concept design that they have in mind.

Bibliography

- [1] VTOL <https://en.wikipedia.org/wiki/VTOL>, January 2023. [Online; access 08-01-2023]
- [2] The ((Quiet)) Electric VTOL Revolution. <https://evtol.news/news/the-quiet-electric-vtol-revolution>, March/April 2020. [Online; access 08-01-2023]
- [3] Focke-Wulf Fw 61. https://en.wikipedia.org/wiki/Focke-Wulf_Fw_61, 22 September 2022. [Online; access 08-01-2023]
- [4] Boeing: Autonomous Flying Taxi: EVTOL Unmanned Solar Aircraft System. <https://www.boeing.com/features/frontiers/2019/autonomous-flying-vehicles/index.page>, 2019. [Online; access 08-01-2023]
- [5] CityAirbus NextGen - Urban Air Mobility - Airbus. <https://www.airbus.com/en/innovation/zero-emission/urban-air-mobility/cityairbus-nextgen>, 24 June 2021. [Online; access 08-01-2023]
- [6] NASA Electric Vertical Takeoff and Landing (eVTOL) Aircraft Technology for Public Services – A White Paper - NASA Technical Reports Server (NTRS). <https://ntrs.nasa.gov/citations/20205000636>, 1 August 2021. [Online; access 08-01-2023]
- [7] Joby Aviation. <https://www.jobyaviation.com/>. [Online; access 08-01-2023]
- [8] Lilium Air Mobility. <https://lilium.com/>. [Online; access 08-01-2023]
- [9] Volocopter brings urban air mobility to life. <https://www.volocopter.com/>. [Online; access 08-01-2023]
- [10] Ansys Student Versions | Free Student Software Downloads. <https://www.ansys.com/academic/students>. [Online; access 08-01-2023]
- [11] SOLIDWORKS. <https://www.solidworks.com/>. [Online; access 08-01-2023]
- [12] Snorri Gudmundsson. General Aviation Aircraft Design: Applied Methods and Procedures. Embry-Riddle Aeronautical University, 2014.
- [13] Aerodynamic Lift and Drag and the Theory of Flight. https://www.mpoweruk.com/flight_theory.htm. [Online; access 09-01-2023]
- [14] Lift (force). [https://en.wikipedia.org/wiki/Lift_\(force\)](https://en.wikipedia.org/wiki/Lift_(force)), January 2023. [Online; access 09-01-2023]
- [15] Aerodynamic Drag – The Physics Hypertextbook. <https://physics.info/drag/>, 2021. [Online; access 09-01-2023]

- [16] What is Drag? - Glenn Research Center | NASA.
<https://www1.grc.nasa.gov/beginners-guide-to-aeronautics/what-is-drag/>,
22 July 2022. [Online; access 09-01-2023]
- [17] John D. Anderson, Jr. Fundamentals of Aerodynamics, Third Edition.
University of Maryland, 2001.
- [18] Egbert Torenbeek with a foreword by H. Wittenberg. Synthesis of Subsonic
Airplane Design. Delft University, 1982.
- [19] ENGINEERING (Aerospace/Civil/Mechanical): Airfoil Nomenclature.
<https://gateengineeringbooksnotes.blogspot.com/2016/01/airfoil-nomenclature.html>. [Online; access 09-01-2023]
- [20] Airfoil Tools. <http://airfoiltools.com/>. [Online; access 10-01-2023]
- [21] Search and Rescue (SAR) | SKYbrary Aviation Safety.
<https://skybrary.aero/articles/search-and-rescue-sar>.
[Online; access 10-01-2023]
- [22] HEMS Safety Risks | SKYbrary Aviation Safety.
<https://www.skybrary.aero/articles/hems-safety-risks>.
[Online; access 10-01-2023]
- [23] Guillermo Von Arend. Main wing study and design for ONAerospace
eVTOL aircraft. Universitat Politècnica de Catalunya, 2023.
- [24] Amine Darkaoui. ONAerospace eVTOL aircraft concept - V-tail study and
design. Universitat Politècnica de Catalunya, 2023.
- [25] Sikorsky Recognizes Bristow and the UK Maritime and Coastguard Agency
for Excellence in Lifesaving Achievement. <https://www.prnewswire.com/news-releases/sikorsky-recognizes-bristow-and-the-uk-maritime-and-coastguard-agency-for-excellence-in-lifesaving-achievement-300297921.html>, 29 June
2018. [Online; access 10-01-2023]
- [26] Centre of Gravity(CG) | SKYbrary Aviation Safety.
<https://skybrary.aero/articles/centre-gravitycg>. [Online; access 14-01-2023]
- [27] aerodynamics - How does airfoil affect the coefficient of lift vs. AOA slope?
<https://aviation.stackexchange.com/questions/86268/how-does-airfoil-affect-the-coefficient-of-lift-vs-aoa-slope>, 31 March 2021. [Online; access 14-01-2023]
- [28] Bjorn's Corner: Pitch stability, Part 3 - Leeham News and Analysis.
<https://leehamnews.com/2018/12/07/bjorns-corner-pitch-stability-part-3/>,
7 December 2018. [Online; access 14-01-2023]

[29] In the C_l vs C_d graph, Why the drag coefficient decreases initially with the small increment in lift coefficient? - Aviation Stack Exchange.

<https://aviation.stackexchange.com/questions/70721/in-the-cl-vs-cd-graph-why-the-drag-coefficient-decreases-initially-with-the-sma>,

16 October 2019. [Online; access 14-01-2023]

[30] Aerodynamic efficiency as a function of the angle of attack.

https://www.researchgate.net/figure/Aerodynamic-efficiency-as-a-function-of-the-angle-of-attack_fig3_317264076. [Online; access 14-01-2023]

[31] Piper PA-28-140 Cherokee - Untitled | Aviation Photo #1021509.

<https://www.airliners.net/photo/Untitled/Piper-PA-28-140-Cherokee/1021509>,

5 June 2005. [Online; access 14-01-2023]

[32] De Havilland Canada DHC-4 Caribo.

https://en.wikipedia.org/wiki/De_Havilland_Canada_DHC-4_Caribou ,

28 December 2022. [Online; access 14-01-2023]

[33] Y+ Wall Distance Estimation. <https://www.cfd-online.com/Tools/yplus.php> ,

[Online; access 04-02-2023]

[34] Best Practice: Scale-Resolving Simulations in Ansys CFD.

<https://www.ansys.com/resource-center/technical-paper/best-practice-scale-resolving-simulations-in-ansys-cfd>,

November 2015. [Online; access 04-02-2023]